Geol. Mag. **156** (*3*), *2019, pp. 485–509* © *Cambridge University Press 2017*
doi:10.1017/S0016756817000875

A lifetime of the Variscan orogenic plateau from uplift to collapse as recorded by the Prague Basin, Bohemian Massif

FRANTIŠEK VACEK*‡ & JIŘÍ ŽÁK‡†

*Department of Mineralogy and Petrology, National Museum, Václavské náměstí 68, Prague, 11579, Czech Republic
‡Institute of Geology and Paleontology, Faculty of Science, Charles University, Albertov 6, Prague, 12843, Czech Republic

(*Received* 10 May 2017; *accepted* 15 September 2017; *first published online* 10 November 2017)

Abstract – The Ordovician to Middle Devonian Prague Basin, Bohemian Massif, represents the shallowest crust of the Variscan orogen corresponding to *c.* 1–4 km palaeodepth. The basin was inverted and multiply deformed during the Late Devonian to early Carboniferous Variscan orogeny, and its structural inventory provides an intriguing record of complex geodynamic processes that led to growth and collapse of a Tibetan-type orogenic plateau. The northeastern part of the Prague Basin is a simple syncline cross-cut by reverse/thrust faults and represents a doubly vergent compressional fan accommodating *c.* 10–19 % ~NW–SE shortening, only minor syncline axis-parallel extension and significant crustal thickening. The compressional structures were locally overprinted by vertical shortening, kinematically compatible with ductile normal shear zones that exhumed deep crust in the orogen's interior at *c*. 346–337 Ma. On a larger scale, the deformation history of the Prague Syncline is consistent with building significant palaeoelevation during Variscan plate convergence. Based on a synthesis of finite deformation parameters observed across the upper crust in the centre of the Bohemian Massif, we argue for a differentiated within-plateau palaeotopography consisting of domains of local thickening alternating with topographic depressions over lateral extrusion zones. The plateau growth, involving such complex three-dimensional internal deformations, was terminated by its collapse driven by multiple interlinked processes including gravity, voluminous magma emplacement and thermal softening in the hinterland, and far-field plate-boundary forces resulting from the relative dextral motion of Gondwana and Laurussia.

Keywords: basin inversion, Bohemian Massif, continental collision, gravitational collapse, orogenic plateau, Teplá–Barrandian Unit

1. Introduction

Spatial and temporal variations in style and intensity of deformation of orogenic upper crust, also referred to as the orogenic 'lid' or 'suprastructure', have long been recognized as an important marker of evolution of collisional orogenic belts (e.g. de Sitter & Zwart, 1960; Zwart, 1967; Murphy, 1987; Culshaw, Beaumont & Jamieson, 2006; Jamieson & Beaumont, 2013). Recently, several end-member models of collisional orogens have been postulated on the basis of integration of geophysical, petrological and structural data with numerical and analogue modelling, making specific predictions as to how the upper orogenic crust should internally deform and/or be vertically and horizontally displaced during plate convergence (e.g. Beaumont, Hamilton & Fullsack, 1996; Beaumont *et al*. 2001; Lister & Foster, 2009; Beaumont, Jamieson & Nguyen, 2010; Graveleau, Malavieille & Dominguez, 2012; Vanderhaeghe, 2012; Jamieson & Beaumont, 2013; Bajolet *et al.* 2015). This issue has been extensively debated in the case of the still tectonically active Tibetan Plateau, where several competing models were formulated (see, e.g., Yin & Harrison, 2000; DeCelles, Robinson & Zandt, 2002; Johnson, 2002; Royden, Burchfiel & van der Hilst, 2008; Searle *et al.* 2011; Styron, Taylor & Murphy, 2011; Lease *et al.* 2012; Li *et al.* 2015; Zuza, Cheng & Yin, 2016 for overviews and discussions) invoking (1) distributed moderate shortening and vertical thickening of the whole lithosphere, (2) intracontinental subduction with significant shortening and thickening of the overriding upper plate, (3) continental underthrusting with no internal shortening but uplift of the overriding plate as a rigid body, and (4) plateau uplift supported by mid- to lower-crustal channel flow without internal deformation of the upper crust. These models show that the three-dimensional deformational histories of orogenic plateaus are likely to be complex, with a variable proportion of crustal shortening, thickening and surface uplift, and lateral extrusion. Importantly, the magnitude and spatio-temporal migration of upper-crustal shortening should reflect, and may thus be used to decipher, deeper processes that shaped the orogen on a lithospheric scale. Another interesting issue in this context is how the intrinsic properties of the upper crust, such as its pre-collisional thickness, tectonic inheritance and thermal–mechanical properties influence (and complicate) the finite deformation pattern.

†Author for correspondence: jirizak@natur.cuni.cz

The potential of the upper crust to record collisional processes on a lithospheric scale is particularly appealing in ancient orogenic belts. Owing to a late-stage isostatic re-equilibration, large portions of these 'fossil' orogens are made up of the exhumed lower to middle crust ('infrastructure') where the early structural record of plate convergence has been pervasively obliterated and thus the amount of crustal shortening is difficult to evaluate. Hence, the preserved upper-crustal fragments may provide the missing key information on the development of an orogen.

The Variscan orogen of Western and Central Europe is an excellent setting to examine the upper-crustal response to plate convergence and collisions (Fig. 1a). The orogen developed as a broad collision zone during protracted convergence of the northerly Laurussia (Old Red Continent) and southerly Gondwana supercontinents, at the expense of the Rheic Ocean and other minor oceanic domains, resulting in the assembly of Pangaea during Late Palaeozoic times (see, e.g., Winchester, 2002; Franke, 2006, 2014; Kroner & Romer, 2013; Stampfli *et al.* 2013 for reviews). In terms of dimensions, kinematics, thermal regime and overall evolution, the Variscan belt is broadly comparable to the modern Alpine–Himalayan system (e.g. Dörr & Zulauf, 2010; Maierová *et al.* 2016 and references therein). As the Variscan belt had undergone a complete orogenic cycle from initial convergence to post-convergent collapse, it could also be used to predict the fate of the still active orogens in the geologic future. Indeed, a vigorous debate has recently centred on the evolution of palaeotopography in the Variscan belt during Devonian to Carboniferous times. Two main opposing views suggest either the presence of a high-elevation Tibetan-style plateau (e.g. Becq-Giraudon, Montenat & Van Den Driessche, 1996; Zulauf *et al.* 2002; Dörr & Zulauf, 2010, 2012) or generally low topography except for narrow strongly deformed belts within the orogen (e.g. Franke, 2012, 2014). This issue has been hotly debated and, in the light of the preceding discussion, may be addressed by analysis of finite deformation patterns of the Variscan upper crust.

Excluding the extensive foreland basins, only a few smaller fragments of upper crust have been preserved along the Variscan belt (Ossa Morena, Northern Armorican Massif, Saxothuringian Unit, Teplá–Barrandian Unit; Fig. 1a). This study examines the Teplá–Barrandian Unit, Bohemian Massif (Fig. 1b), the easternmost of these upper-crustal fragments positioned in a hangingwall with respect to the surrounding, mostly high-grade metamorphic complexes (Fig. 1b). We concentrate on the central portion of the Teplá–Barrandian Unit where its low-grade Cadomian basement is unconformably overlain by the Ordovician to Middle Devonian volcano-sedimentary successions of the Prague Basin (Fig. 1b). In terms of palaeodepth, the basin represents the shallowest crust within the Variscan orogen and is superbly exposed, allowing rigorous analysis of its architecture and deformation. As modern systematic structural studies are lacking, we first characterize folds and faults in this basin in detail, estimate the amount of finite shortening and synthesize our data into a new tectonic model. We then interpret the tectonic evolution of the Prague Basin and evaluate the bulk three-dimensional deformation of orogenic upper crust in the Bohemian Massif. Finally, we discuss the broad implications of our model for the evolution of palaeotopography, crustal thickening and collapse during the Variscan orogeny.

2. Development and stratigraphy of the Prague Basin

The Prague Basin developed on top of the pervasively deformed Cadomian (late Neoproterozoic to early Cambrian) accretionary wedge and also overlaps middle to late Cambrian continental–marine basins and late Cambrian volcanic complexes (Figs 1b, 2; e.g. Havlíček, 1980, 1981; Štorch, Fatka & Kraft, 1993; Chlupáč, 1993; Chlupáč *et al.* 1998; Fatka & Mergl, 2009 and references therein). Altogether, these units formed at the northern margin of West Gondwana during protracted oceanic subduction and record a continuum of processes involving growth of an active plate margin and its decay and inversion to a volcanic passive margin during ~650–490 Ma (e.g. Dörr *et al.* 2002; Drost *et al.* 2004, 2011; Sláma *et al.* 2008; Fatka & Mergl, 2009; Hajná, Žák & Kachlík, 2011; Hajná, Žák & Dörr, 2017). The Prague Basin presumably initiated as a narrow fault-bounded graben and was interpreted as part of the extensive peri-Gondwana passive margin in the southern realms of the Rheic Ocean (e.g. Patočka, Pruner & Štorch, 2003; Patočka & Štorch, 2004; Aifa *et al.* 2007; Žák, Kraft & Hajná, 2013).

The basin is filled with a continuous volcano-sedimentary marine succession ranging from the lowermost Ordovician (Tremadocian) to Middle Devonian (Givetian) with a minimum and maximum cumulative thicknesses of *c.* 1200 and 5100 m (Figs 2–11; see Chlupáč, 1988; Chlupáč, 1993; Chlupáč *et al.* 1998; Štorch, Fatka & Kraft, 1993; Fatka & Mergl, 2009 for detailed overviews). The succession consists of: (1) Ordovician siliciclastic rocks (shales, siltstones, sandstones; up to ~3700 m thick in total) interpreted as cold-water passive-margin, continental shelf deposits (e.g. Havlíček, 1982; Fatka *et al.* 1995; Mikuláš, 1998). Dropstone horizons in the uppermost stratigraphical levels (Fig. 7f) indicate that the Prague Basin was within the reach of peri-Gondwana continental glaciers during Late Ordovician times (Hirnantian; Štorch, 1986, 1990, 2006; Brenchley & Štorch, 1989). (2) The Ordovician siliciclastic rocks are conformably overlain by Silurian tuffitic and graptolite black shales (Fig. 8a), which were deposited in an oxygen-poor environment and pass upwards into warm-water carbonates (maximum total thickness of the Silurian is ~630 m (e.g. Kříž, 1991, 1992; Lehnert *et al.* 2007; Manda *et al.* 2012; Štorch & Frýda, 2012; Frýda & Frýdová, 2014; Štorch *et al.* 2016). (3) The carbonate deposition continued across the Silurian–Devonian

https://doi.org/10.1017/S0016756817000875 Published online by Cambridge University Press

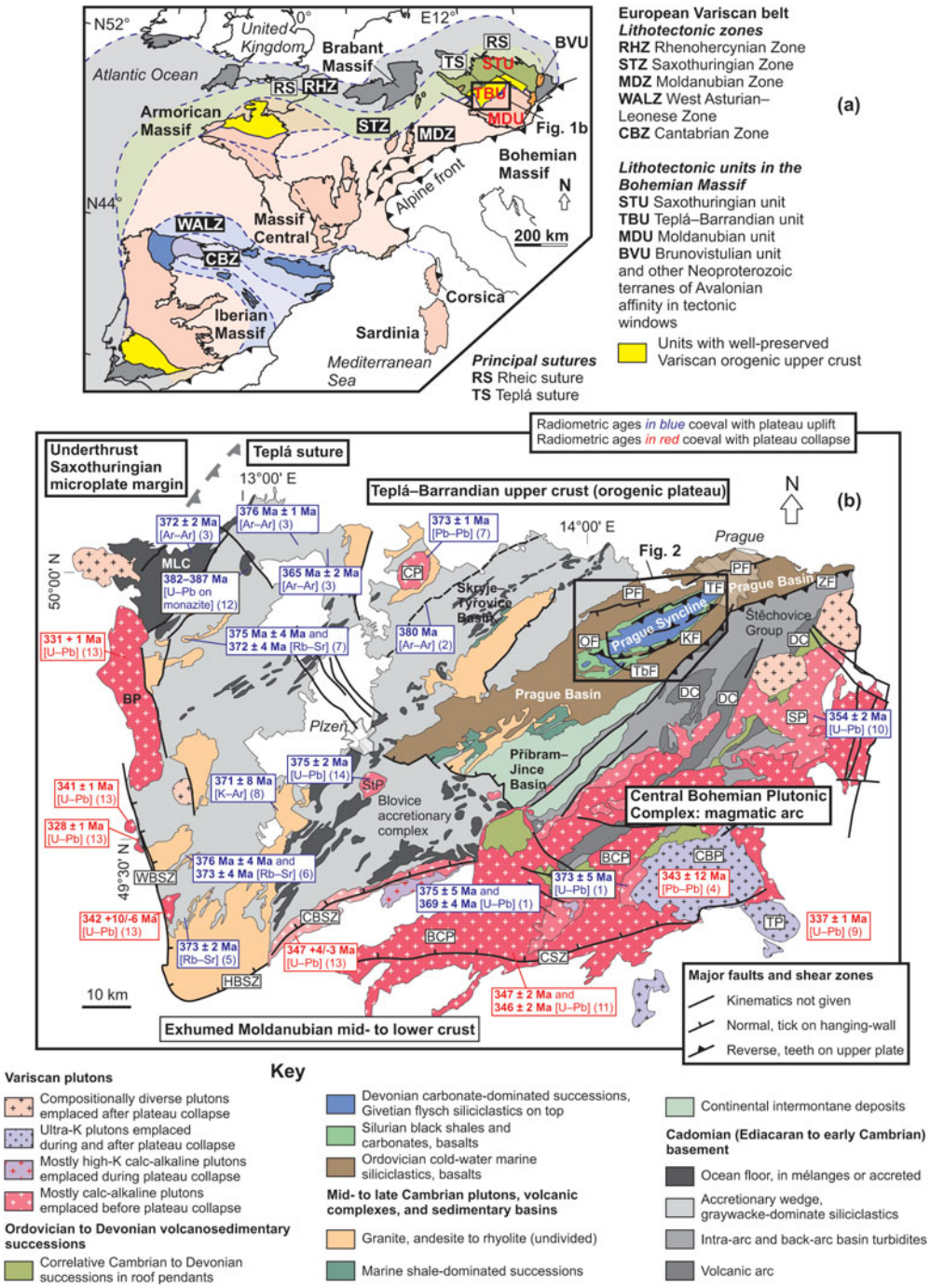

Figure 1. (Colour online) (a) Overview geological map showing basement outcrop areas and principal lithotectonic zones and sutures of the Variscan orogenic belt in Europe. The Bohemian Massif is the easternmost inlier of the orogen. Upper-crustal Cadomian basement units (including the Teplá–Barrandian Unit) are highlighted in yellow. Compiled from Winchester (2002) and Martínez Catalán (2011). (b) Simplified geological map of the Teplá–Barrandian Unit made up of the Cadomian basement, Cambro–Ordovician igneous complexes, Early Palaeozoic basins and Late Devonian to early Carboniferous plutons. Published geochronological data were selected to constrain the Variscan evolution and are grouped into those coeval with orogenic horizontal shortening and plateau growth and those coeval with plateau collapse ('elevator tectonics' of Dörr & Zulauf, 2010). The map was redrafted from the 1:500 000 geological map of the Czech Republic, published by the Czech Geological Survey in 2007. Source of geochronological data: (1) Košler, Aftalion & Bowers (1993); (2) Dallmeyer & Urban (1994); (3) Dallmeyer & Urban (1998); (4) Holub, Cocherie & Rossi (1997); (5) Košler *et al.* (1997); (6) Glodny *et al.* (1998); (7) Venera, Schulmann & Kroner (2000); (8) Zulauf (2001 and references therein); (9) Janoušek & Gerdes (2003); (10) Janoušek *et al.* (2004); (11) Janoušek, Wiegand & Žák (2010); (12) Timmermann *et al.* (2006); (13) Dörr & Zulauf (2010); (14) Žák *et al.* (2011). Lithological and tectonic units: BCP – Blatná composite pluton; BP – Bor pluton; CBP – Čertovo břemeno pluton; CBSZ – Central Bohemian shear zone; CP – Čistá pluton; CSZ – Červená shear zone; DC – Davle volcanic complex; HBSZ – Hoher Bogen shear zone; KF – Koda Fault; MLC – Mariánské Lázně complex; OF – Očkov Fault; PF – Prague Fault; SP – Sázava pluton; StP – Štěnovice pluton; TbF – Tobolka Fault; TF – Tachlovice Fault; TP – Tábor pluton; WBSZ – West Bohemian shear zone; ZF – Závist Fault.

https://doi.org/10.1017/S0016756817000875 Published online by Cambridge University Press

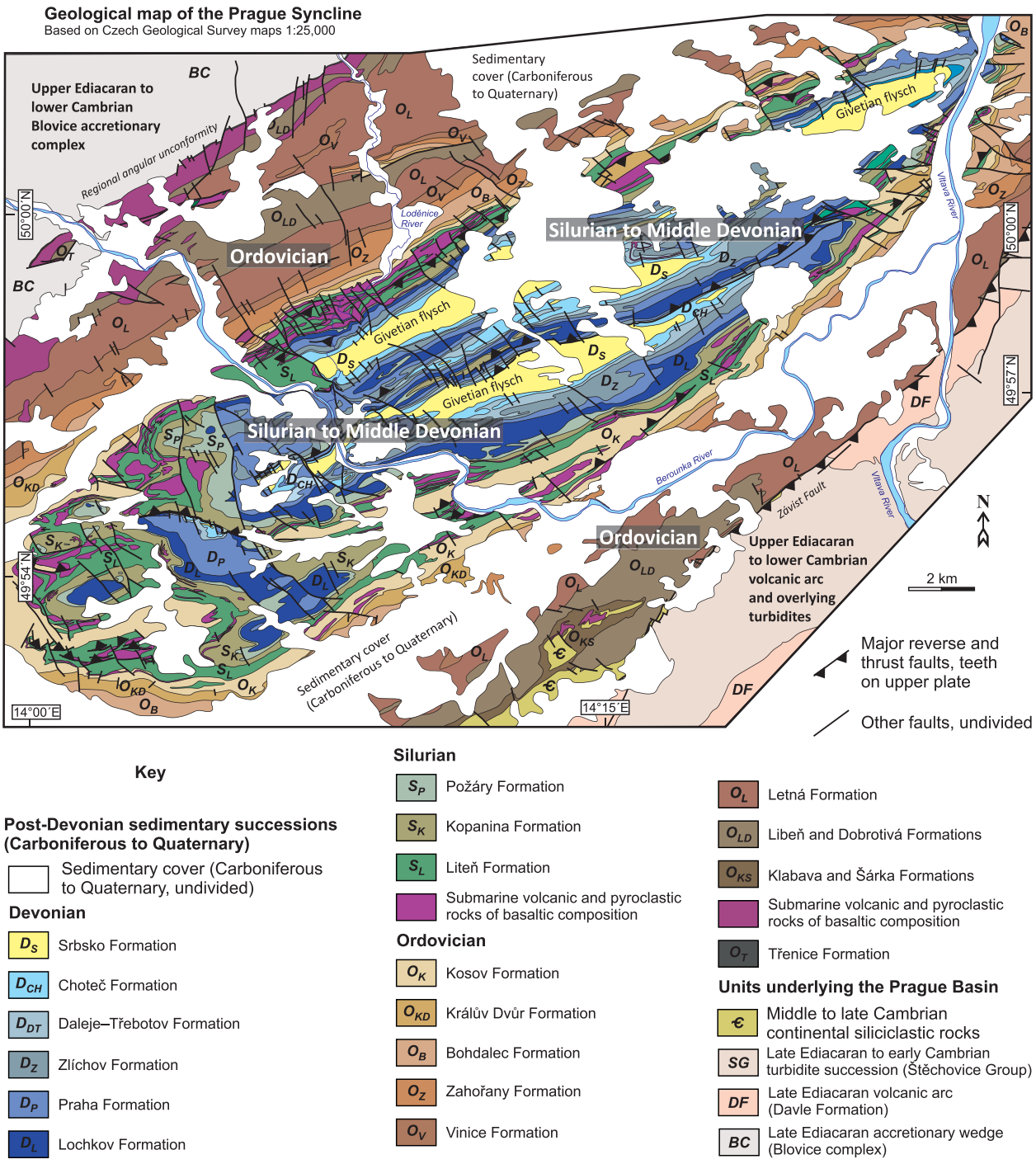

Figure 2. (Colour online) Geological map of the Prague Syncline and adjacent Cadomian basement. The map was compiled and modified from the Czech Geological Survey maps 1:25 000, sheets 12-243 Praha-sever, 12-411 Beroun, 12-412 Rudná, 12-413 Králův Dvůr, 12-414 Černošice, 12-421 Praha-jih, 12-423 Davle, 12-431 Hostomice and 12-432 Mníšek pod Brdy.

boundary and resulted in an up to ~570 m thick (in total) package of Lower to Middle Devonian warm-water carbonates (Fig. 8b) including reef and carbonate platform facies (e.g. Chlupáč, 2003; Koptíková *et al.* 2010; Ferrová, Frýda & Lukeš, 2012; Vodrážková *et al.* 2013). (4) Lastly, the carbonate succession is capped by ~250 m thick Givetian flysch siliciclastic rocks (shales, siltstones, sandstones), which mark the onset of basin inversion during the initial stages of the Variscan orogeny (Fig. 8c; Kukal & Jäger, 1988; Strnad & Mihaljevič, 2005). Moreover, the whole Ordovician to Middle Devonian succession is interfingered with submarine basaltic volcanic complexes and sills (Fig. 8a), with the main peaks of the volcanic activity in Middle Ordovician (Floian–Sandbian) and early to late Silurian (Wenlock–Ludlow; Fig. 3) times.

In accordance with palaeomagnetic data, the basin succession records an equator-ward drift of the Prague Basin from a latitude of *c.* 40° S in late Cambrian times to subtropical latitudes (*c.* 10–20° S) in Middle Devonian times (e.g. Krs *et al.* 1987; Tait, Bachtadse & Soffel, 1994, 1995; Krs, Pruner & Man, 2001; Aifa

https://doi.org/10.1017/S0016756817000875 Published online by Cambridge University Press

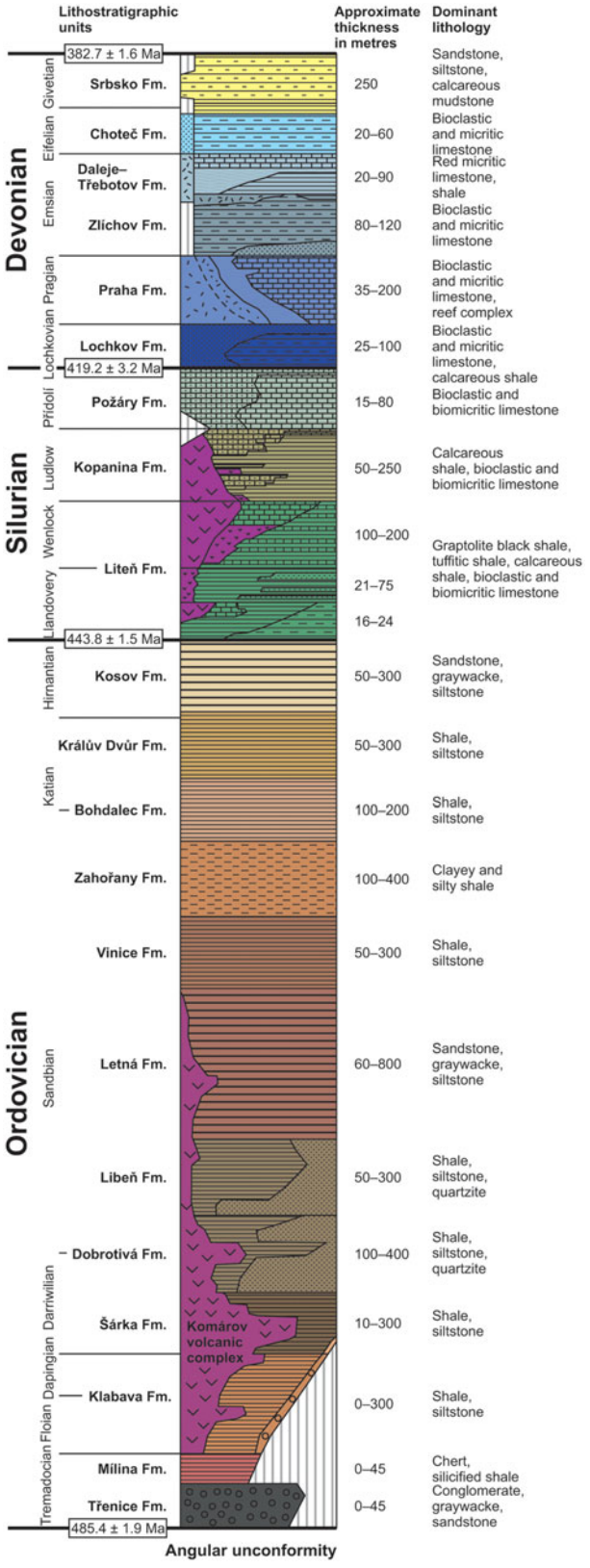

Figure 3. (Colour online) Stratigraphical chart summarizing lithostratigraphy of the Ordovician to Middle Devonian successions of the Prague Basin. Compiled from Chlupáč (1993) and Chlupáč *et al*. (1998). Numerical ages are according to the International Chronostratigraphic Chart published in 2016 (http://www.stratigraphy.org).

et al. 2007; Tasáryová *et al.* 2014). It remains a matter of debate whether the Teplá–Barrandian Unit, including the Prague Basin, remained attached to Gondwana as a part of its extended passive margin or whether it was completely detached and became a far-travelled continental terrane isolated within the Rheic Ocean during Early Palaeozoic times (see, e.g., Paris & Robardet, 1990; Robardet, 2003; Fatka & Mergl, 2009; Servais & Sintubin, 2009; Žák & Sláma, 2017 for discussions).

During the Variscan plate convergence, the northwesterly oceanic domain (Saxothuringian Ocean) followed by the Saxothuringian continental margin were progressively subducted beneath the overriding Teplá–Barrandian upper crust (from >380 Ma to ∼340 Ma), resulting in its overall ∼NW–SE to ∼WNW–ESE horizontal shortening (e.g. Zulauf, 1997, 2001; Konopásek & Schulmann, 2005; Schulmann *et al.* 2009, 2014; Žák *et al.* 2009; Franěk *et al.* 2011; Hajná *et al.* 2012). The Prague Basin was inverted, uplifted and multiply deformed (e.g. Havlíček, 1963, 1981; Chlupáč *et al.* 1998; Melichar, 2004; Röhlich, 2007 and references therein) in response to this crustal shortening. The existing apatite fission-track ages indicate maximum burial of the basin during Late Devonian to early Carboniferous times (Glasmacher, Mann & Wagner, 2002; Filip & Suchý, 2004) while the fluid inclusion studies estimate a palaeodepth of *c*. 1–4 km, i.e. still within the oil window for the uppermost (Givetian) strata in the basin (e.g. Suchý *et al.* 1996, 2002*a*,*b*, 2010, 2012, 2015; Volk *et al.* 2002; Halavínová, Melichar & Slobodník, 2008).

Importantly, the style and intensity of the Variscan deformation varies along strike of the Prague Basin which, as a result, is divided into two contrasting segments (Fig. 1b). The southwestern segment is made up of Ordovician siliciclastic rocks and is dismembered into a mosaic of fault-bounded blocks. Bedding attitude varies from one block to another from commonly flat to rarely steep. In contrast, the northeastern segment forms a ∼36 km long and ∼16 km wide (at the present-day erosional level) ∼NE–SW-trending syncline with Ordovician siliciclastic rocks in the periphery and Silurian–Devonian predominantly carbonate successions in the core (Figs 1b, 4–6). This northeastern segment is hereinafter referred to as the 'Prague Syncline' and is, together with its Cadomian basement, described in detail below.

3. Lithomechanical layers and structural pattern of the Prague Syncline

Below we describe mesoscopic deformational structures in the Prague Syncline and concentrate on bedding orientation, cleavage, folds, and major reverse and thrust faults. The emphasis is put mostly on structures directly relevant to the Variscan basin inversion and shortening; younger brittle deformation features will be dealt with in a separate paper.

https://doi.org/10.1017/S0016756817000875 Published online by Cambridge University Press

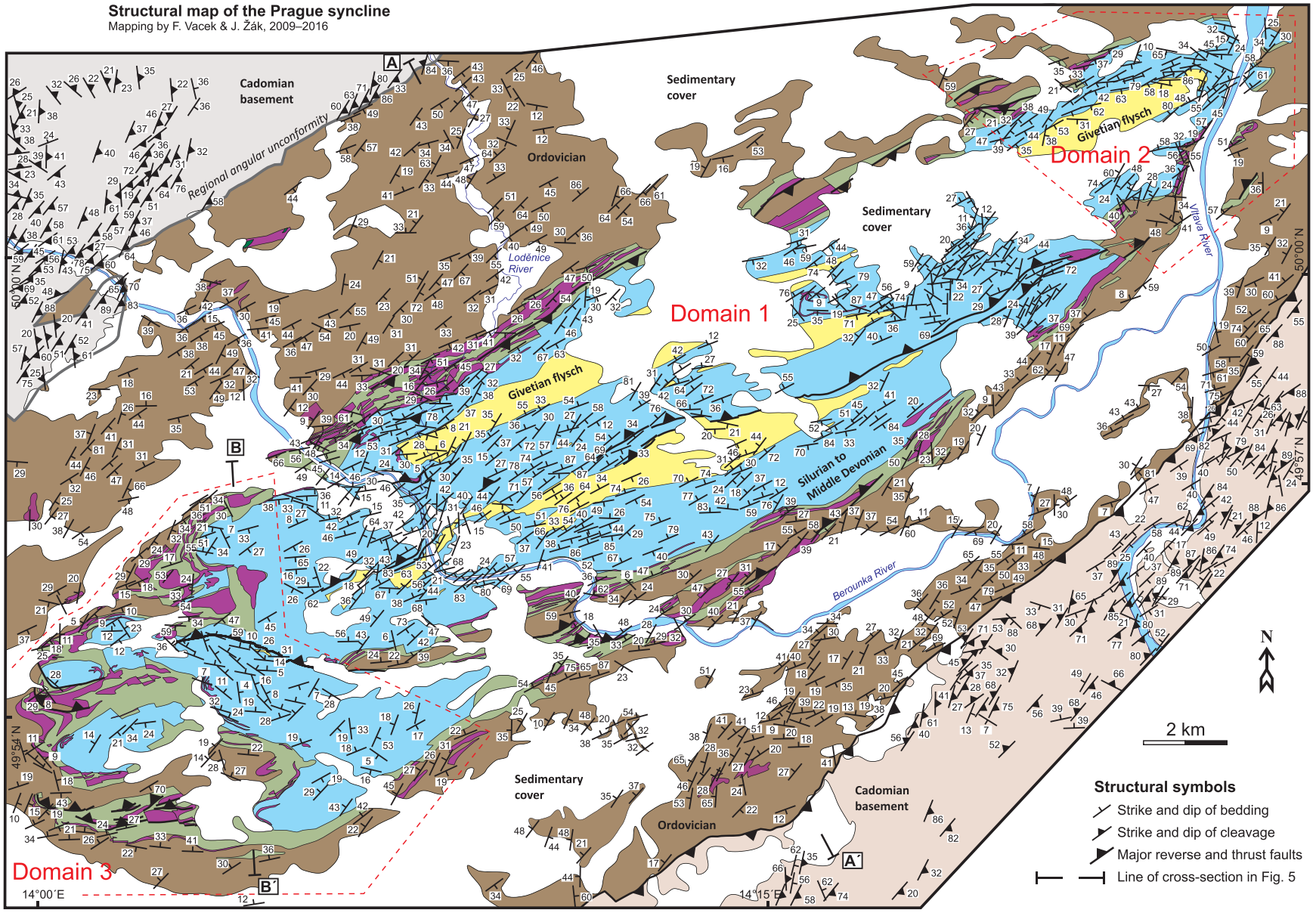

Figure 4. (Colour online) Structural map of the Prague Syncline showing strike and dip of bedding in the four main lithomechanical layers as defined in this study (Cadomian basement, Ordovician siliciclastic rocks, Silurian–Devonian core, Givetian flysch). The base map was derived from Figure 2.

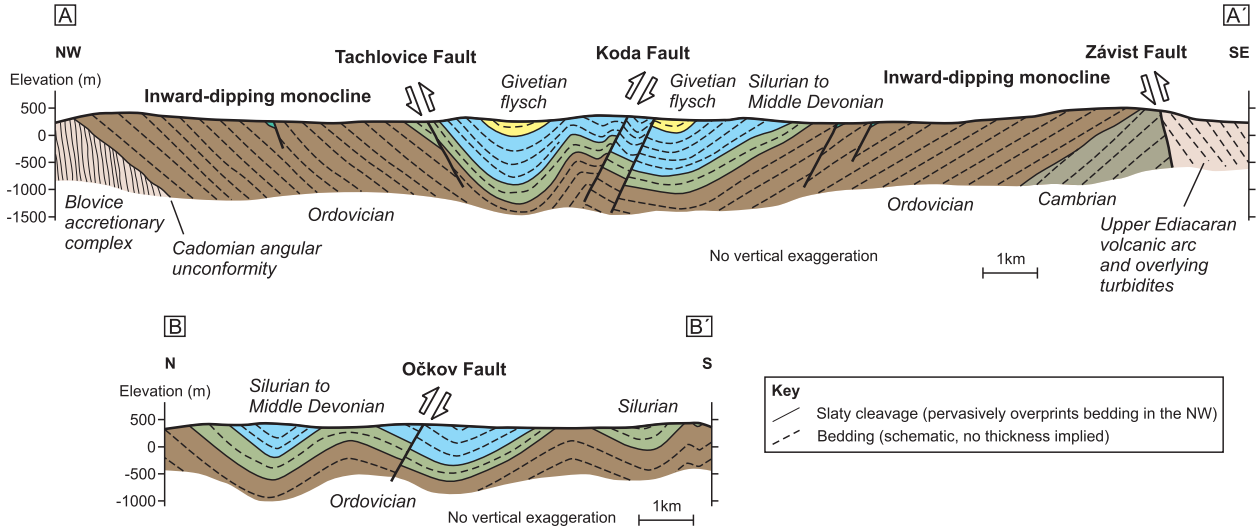

Figure 5. (Colour online) Schematic interpretive cross-sections across the Prague Syncline along lines A–A´and B–B´(see Fig. 4 for location). Note the overall simple structure of the main syncline with limb monoclines made up of the Ordovician siliciclastic rocks in the periphery and smaller-wavelength folds in the Silurian–Devonian core. Cross-sections are based on our field observations and structural data presented in Figure 4.

The main stratigraphical units as described above can be grouped into four first-order lithomechanical layers that differ in thickness and bulk mechanical properties (Figs 4–6) and controlled the large-scale deformation and style of folding and faulting of the Prague Syncline: (1) the strongly anisotropic but lithologically homogeneous Cadomian basement, (2) a thick package of Ordovician siliciclastic rocks in the basin periphery, (3) the inner Silurian–Devonian core dominated by carbonate successions, and (4) Givetian flysch siliciclastic rocks on top. The description of deformational structures will generally follow this scheme.

3.a. Deformational structures in the Cadomian basement

Recent structural studies showed that the Cadomian basement units exposed on both sides of the Prague Basin differ in lithology, age, metamorphic grade, intensity of cleavage development and inferred tectonic setting (see Hajná *et al.* 2010; Hajná, Žák & Kachlík, 2011; Hajná, Žák & Dörr, 2017 for details).

In the northwest, the Prague Basin overlies an exhumed accretionary wedge (the Blovice complex dated at *c.* 635–520 Ma; Figs 1b, 2), which here comprises lithologically uniform (meta-)greywackes and slates that have been weakly metamorphosed under lower-greenschist-facies conditions and affected by an intensely developed slaty cleavage (Fig. 7a). Bedding and primary sedimentary features are commonly disrupted and pervasively obliterated by the cleavage and thus are not macroscopically discernible in most outcrops. The cleavage strikes ~NE and dips gently to moderately to the ~SE; mean dip direction and dip are 116° and 45°, respectively. In a *c.* 1–2 km wide zone along the depositional contact with the overlying Prague Basin, the cleavage progressively steepens and reorients from a ~NW–SE to ~NNE–SSW strike (Figs 4–6). On a stereonet, the cleavage poles define a weak girdle around a subhorizontal ~NE–SW axis; the axis calculated as the minimum eigenvector of the orientation tensor is 037°/11° (Fig. 6). In some places, the cleavage has been folded into metre-scale chevron folds and overprinted by several sets of contractional kink bands.

In contrast, the Cadomian basement adjacent to the SE margin of the Prague Basin is made up of the *c.* 590–560 Ma Davle volcanic arc complex and an overlying *c.* 560–530 Ma flysch-like siliciclastic succession (Štěchovice Group in Fig. 1b; Sláma *et al.* 2008) which underwent very-low-grade anchimetamorphism (Suchý *et al.* 2007) and were only weakly strained during the Variscan orogeny. Bedding is well preserved and only gently tilted (Fig. 7b), dipping moderately to the SE (mean bedding is 137°/33°; dip direction/dip convention is used throughout this paper; Figs 4–6). A weakly developed spaced pressure-solution cleavage cuts across the bedding (Fig. 7b), is steep and strikes ~NNE–SSW to ~NE–SW (mean orientation is 124°/77°; Figs 4, 6).

3.b. Ordovician periphery of the Prague Syncline

The Ordovician siliciclastic successions overlie the Cadomian basement with a pronounced regional angular unconformity apparent from the map (Fig. 4) and well exposed in several outcrops. While this unconformity delineates the northwestern margin of the basin, its southeastern flank is truncated by a major ~NE–SW-trending and ~SE-dipping reverse fault (Závist Fault in Figs 2, 4, 5). This fault thrusts the Cadomian basement over the Ordovician siliciclastic rocks and despite it not being exposed, map-scale relationships and near-fault deformation features

https://doi.org/10.1017/S0016756817000875 Published online by Cambridge University Press

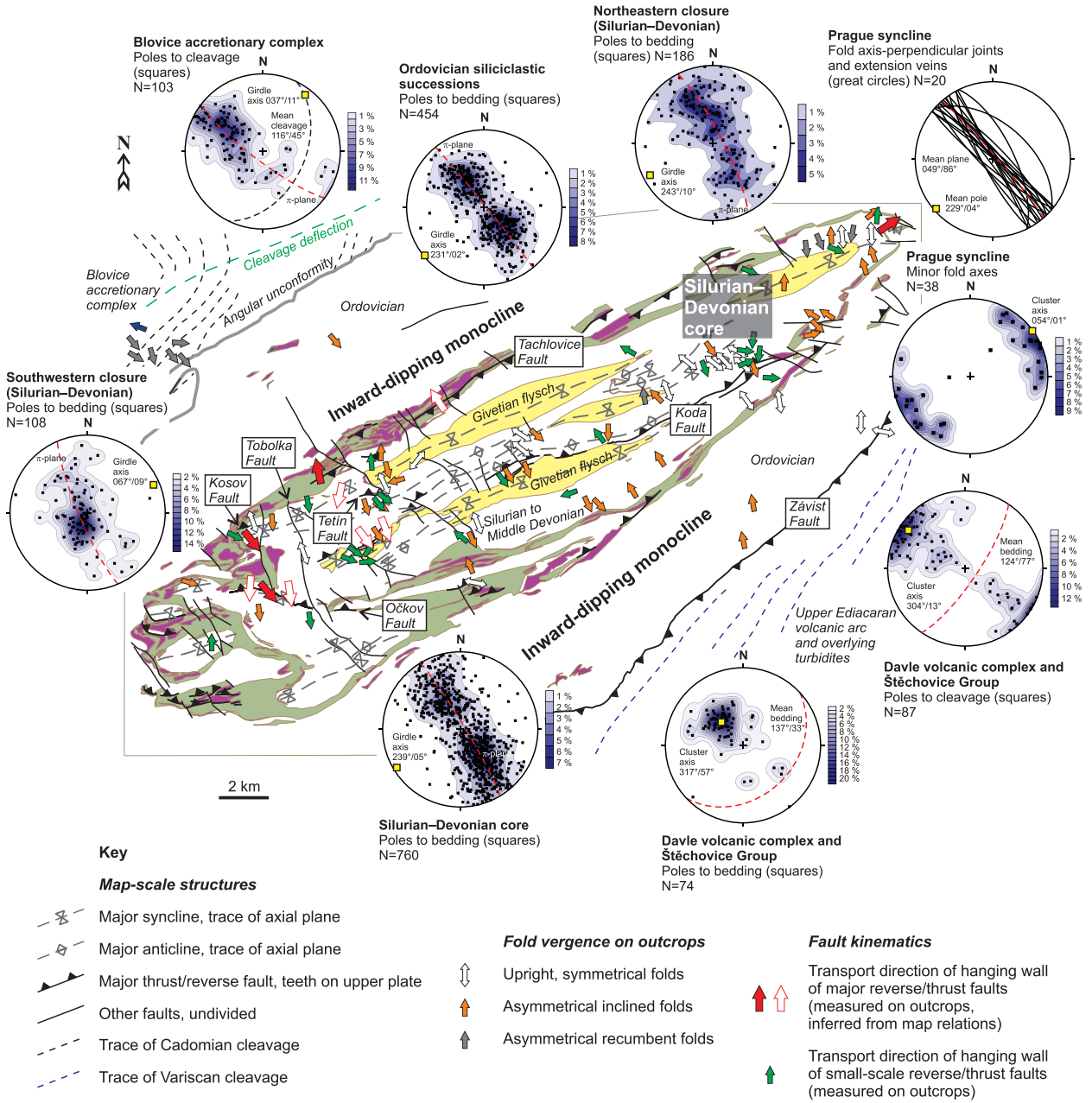

Figure 6. (Colour online) A synthetic tectonic scheme highlighting the large-scale architecture of the Prague Syncline (derived from structural data presented in Figure 4; faults were transferred from Figure 2). Stereonets (equal area projection, lower hemisphere) show orientation of cleavage in the Cadomian basement and bedding in different parts of the syncline. Arrows indicate fold vergence and kinematics of reverse/thrust faults (transport direction of the hangingwall as documented on outcrops). Note the fault kinematics is variable across the syncline.

(dragged bedding and down-dip slickenlines on associated minor fault planes) are consistent with the top-to-the-NW motion of the hangingwall (Fig. 7c–e).

Except for abundant small-scale faults and extremely rare metre-scale buckle folds (mostly along faults; Fig. 7c), the structure of the Ordovician successions is rather uniform. In outcrops, bedding dips at moderate angles (*c.* 40°–50°) to the ~SE in the northwestern limb of the Prague Syncline and to the ~NW in the southeastern limb (Figs 4–6). Both limbs thus represent large-scale inward-dipping monoclines (Figs 4–6). On a stereonet, poles to bedding define a pronounced girdle with two maxima distributed symmetrically about a ~NE–SW-trending axis (Fig. 6; mean is 231°/02°; calculated the same way as above). The Ordovician strata are devoid of any regional cleavage (Fig. 7f), except for local bedding-parallel cleavage in shale interbeds between competent sandstones and spaced cleavage along faults.

3.c. Silurian–Devonian core of the Prague Syncline

Based on the orientation of bedding and fold and fault geometry and kinematics, three distinct structural domains have been identified in this study (Fig. 4): the central part of the Prague Syncline (Domain 1) and

https://doi.org/10.1017/S0016756817000875 Published online by Cambridge University Press

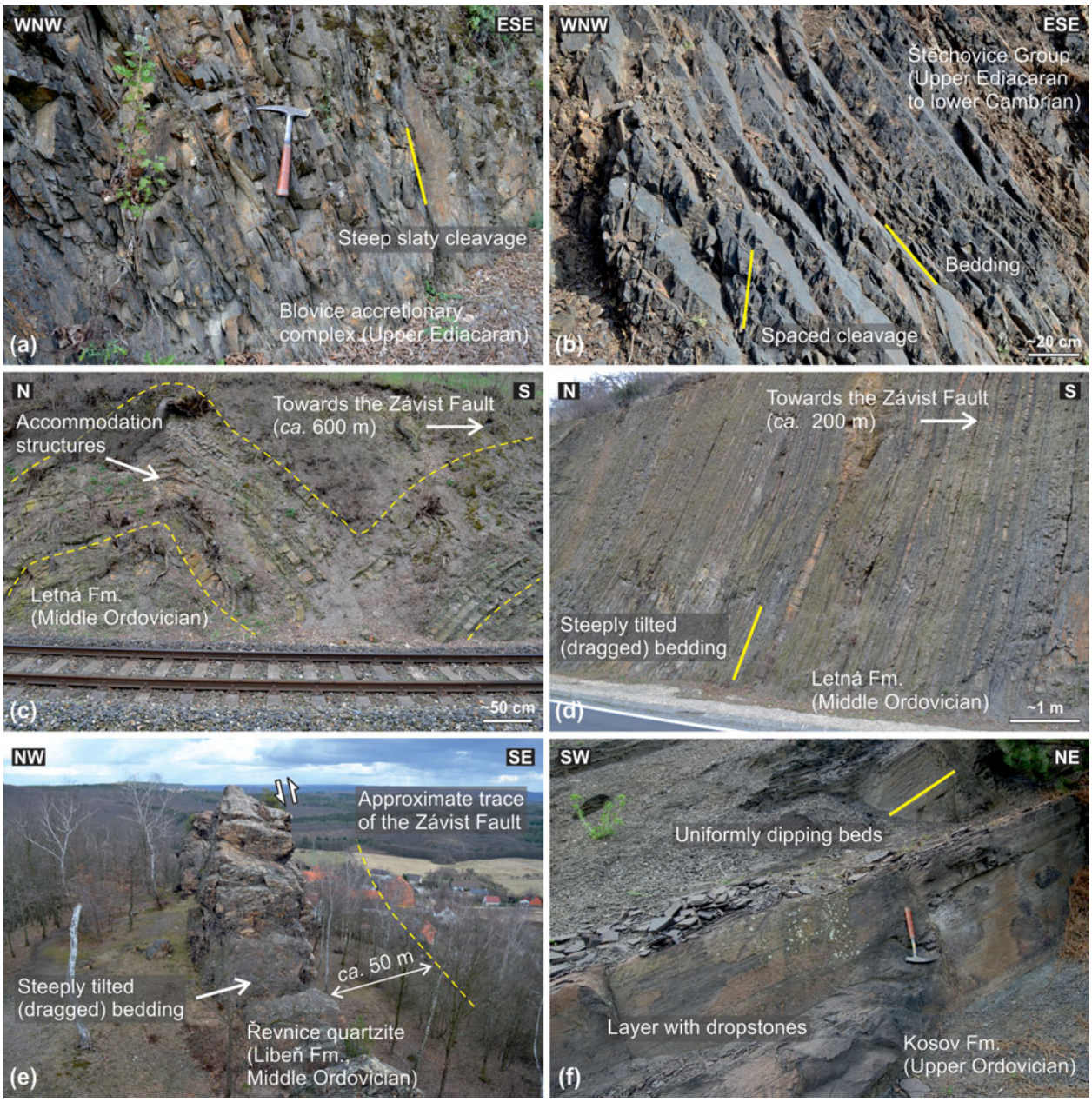

Figure 7. (Colour online) Deformational structures in the Cadomian basement and Ordovician periphery of the Prague Syncline. (a) Steep slaty cleavage in (meta-)greywackes of the Blovice accretionary complex; bedding has been completely obliterated. Hammer for scale is 33 cm long. Railroad cut ~1 km SE of Nižbor, coordinates (WGS84 datum): 49.9995392° N, 14.0166572° E. (b) Well-preserved, moderately dipping bedding cross-cut by weakly developed spaced pressure-solution cleavage; laminated siliciclastic succession of the Štěchovice Group. Road cut ~550 m SW of Strnady, coordinates (WGS84 datum): 49.9425650° N, 14.3869778° E. (c) Metre-scale forced folds developed in rhythmically bedded siliciclastic rocks in the footwall of the Závist Fault (Letná Fm). Railroad cut ~200 m NW of Závist, coordinates (WGS84 datum): 49.9758578° N, 14.3992461° E. (d) Steeply tilted to overturned bedding in the footwall of the Závist Fault (Letná Fm). Road cut ~300 m SW of Závist, coordinates (WGS84 datum): 49.9729150° N, 14.4004425° E. (e) Steeply tilted thick quartzite beds in the footwall several tens of metres below the Závist Fault (Libeň Fm). Černolice, coordinates (WGS84 datum): 49.9131589° N, 14.3033694° E. (f) Only gently tilted Upper Ordovician (Hirnantian) finely laminated siliciclastic rocks containing abundant dropstones (Kosov Fm). The shallow to moderate dip without any metre-scale folds is typical for most of the Ordovician outcrops in the Prague Syncline. Hammer for scale is 33 cm long. Outcrop ~400 m SE of Levín, coordinates (WGS84 datum): 49.9277861° N, 14.0123442° E.

its northeastern and southwestern closures (Domains 2 and 3, respectively).

3.c.1. Domain 1: central part of the syncline

On the map, Domain 1 exhibits a generally simpler structural pattern than both closures of the Prague Syncline and consists of several alternating second-order synclines and anticlines of up to several kilometres wavelength and ~NE–SW-trending subhorizontal axes, locally deflected into a ~WSW–ENE direction (Figs 4, 6). In an axis-perpendicular section (Fig. 5), these kilometre-scale anticlines and synclines are upright, symmetrical to weakly asymmetrical, and

https://doi.org/10.1017/S0016756817000875 Published online by Cambridge University Press

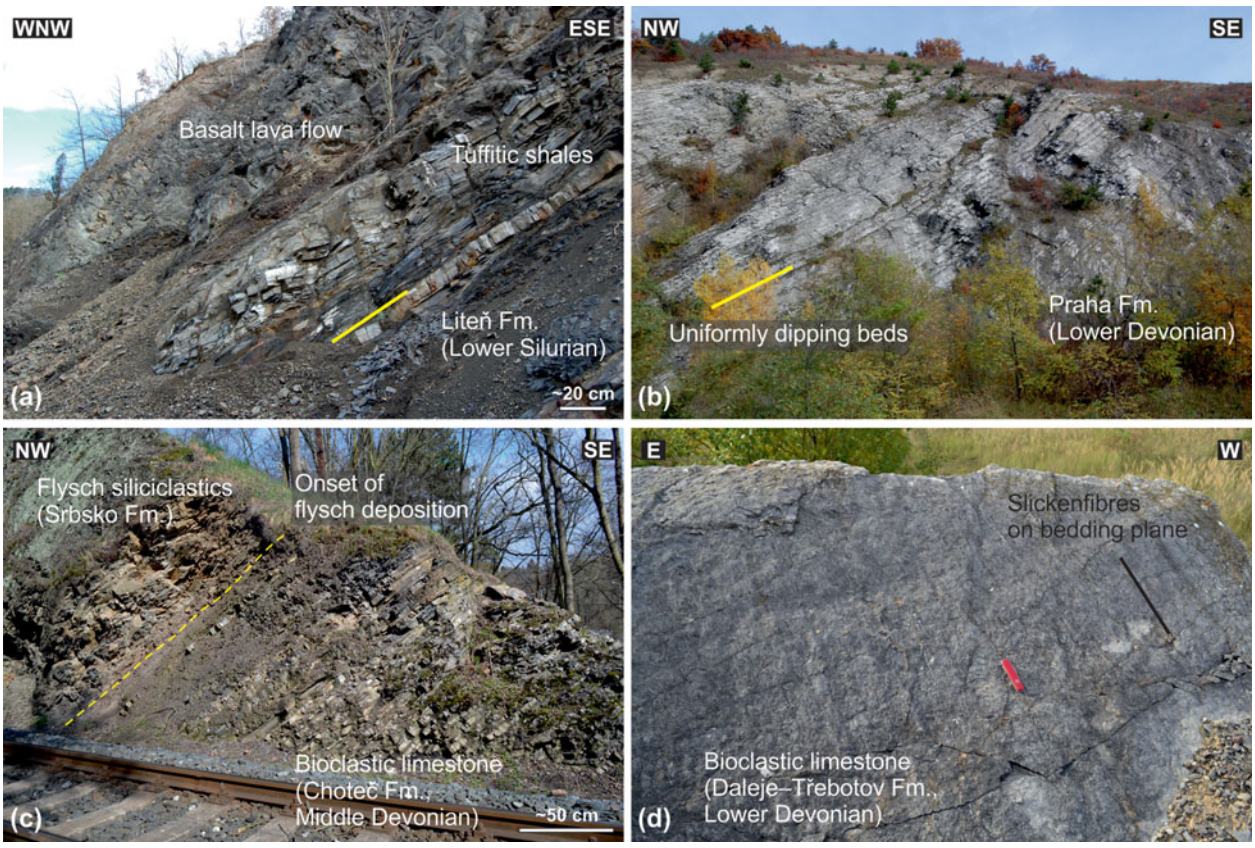

Figure 8. (Colour online) Structural features of the main lithostratigraphical units of the Silurian–Devonian core of the Prague Syncline. Gently to moderately dipping bedding with no minor folds is characteristic for most outcrops. (a) Lower Silurian tuffitic shales overlain by a basaltic lava flow (Liteň Fm). Road cut ~800 m SE of Karlštejn, coordinates (WGS84 datum): 49.9281617° N, 14.1880275° E. (b) Lower Devonian thinly bedded limestones (Praha Fm). Trees in the forefront are *c*. 5 m high. Praha-Radotín, coordinates (WGS84 datum): 49.9941333° N, 14.3435758° E. (c) Base of the Middle Devonian Variscan flysch siliciclastic rocks overlying the carbonate platform limestones (Choteč Fm). Railroad cut, Praha-Hlubočepy, coordinates (WGS84 datum): 50.0389244° N, 14.3957606° E. (d) Down-dip calcite slickenfibres on a limestone bedding plane formed by bedding-parallel slip during folding (Daleje–Třebotov Fm). Swiss Army penknife (9 cm long) for scale. Disused quarry Červený lom ~1.4 km SE of Koněprusy, coordinates (WGS84 datum): 49.9106256° N, 14.0768314° E.

open, with the interlimb angle mostly exceeding 80°–90°. The folds are non-cylindrical (periclinal), as anticlines and synclines exhibit a whaleback and canoe geometry, respectively (Figs 4, 6). This is best documented in synclines cored by Givetian flysch which have inward-plunging axes, i.e. to the SW in their northeastern closures and to the NE in their southwestern closures (Figs 4, 6).

Most outcrops and sections in Domain 1 are dominated by uniformly dipping monoclines which represent limbs of the kilometre-scale folds. Except for several, isolated metre-scale buckle folds, the monoclines are unfolded on smaller scales (Fig. 8a, b). In general, bedding dips either to the ~NW or ~SE at variable, but mostly moderate angles of *c*. 30–50° (Figs 4–6). Down-dip oriented slickenfibres are common on bedding planes (Fig. 8d) as well as locally developed metre-scale duplexes (Fig. 11a). On a stereonet, poles to bedding thus define a pronounced girdle about a ~NE–SW-trending axis (Fig. 6; mean is 239°/05°; calculated the same way as above).

This dominant simple fold style on the kilometre scale (Figs 4–6) becomes only locally more complicated within the lowermost Devonian Lochkov Formation (Fig. 9). This stratigraphical unit consists of *c*. 10–20 cm thick limestone beds alternating with calcareous shale interbeds of approximately the same thickness, which facilitated bedding-parallel slip and thus folding. Abundant metre-scale buckle folds occur here within a tens of metres thick horizon, exposed on several isolated outcrops along the southeastern margin of the Silurian–Devonian core and northeastern closure of the Prague Syncline (Domains 1 and 3; Fig. 9). The folding is disharmonic and fold geometry varies greatly from symmetrical to asymmetrical, isoclinal to open, and upright to recumbent (Fig. 9).

3.c.2. Domains 2 and 3: closures of the Prague Syncline

Both closures of the Prague Syncline differ in lithology and stratigraphy, width and overall architecture (Figs 4, 6). The northeastern closure (Domain 2) includes a complete stratigraphical succession from Silurian to Middle Devonian (Givetian); it is comparatively simple with a narrow hinge zone dismembered by several faults (Figs 4, 6). Bedding orientations are

https://doi.org/10.1017/S0016756817000875 Published online by Cambridge University Press

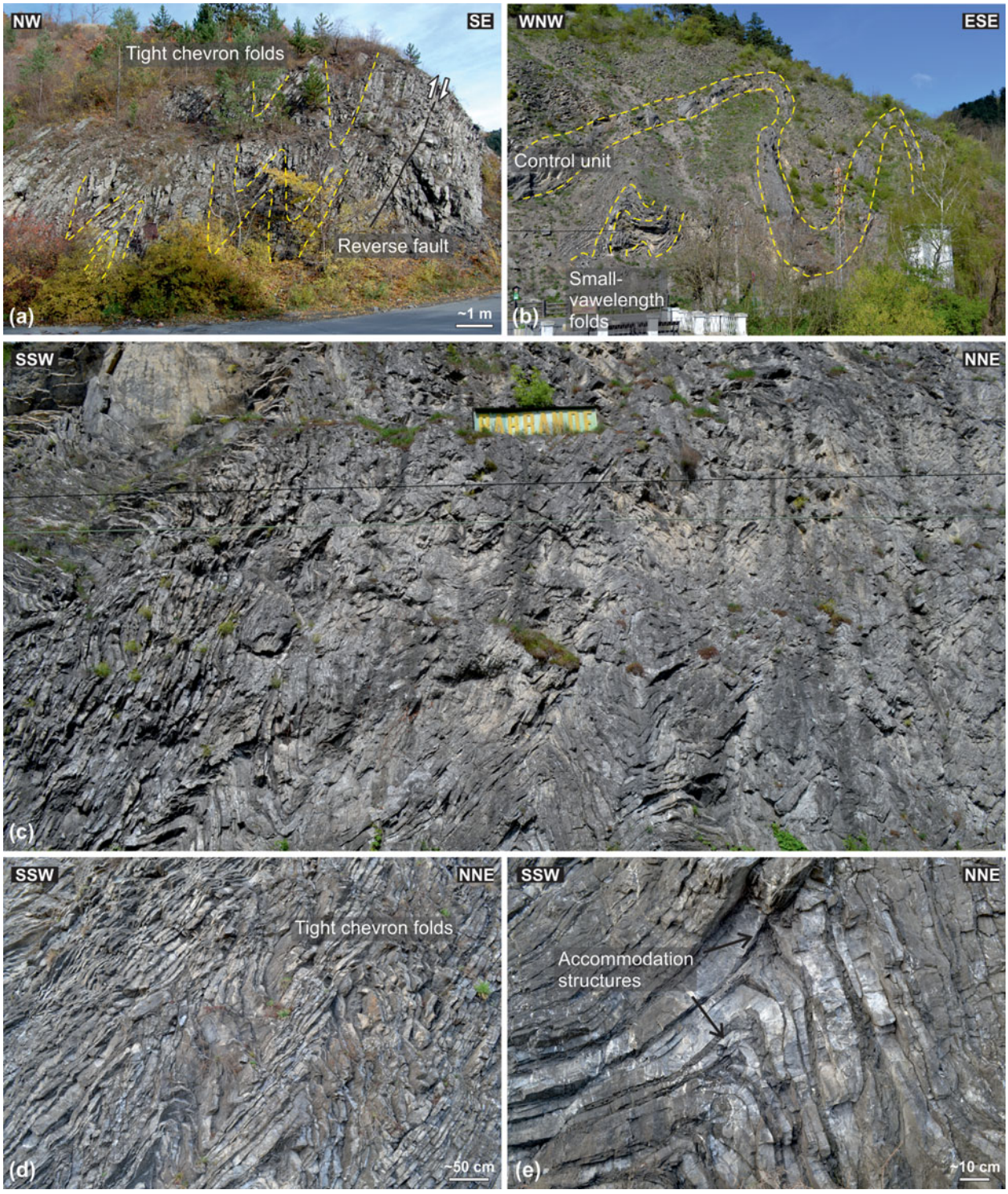

Figure 9. (Colour online) Examples of buckle folds of various geometries and orientations formed within a localized high-strain horizon above the Silurian–Devonian boundary (Lochkov Fm). The intense folding was facilitated by thinly bedded limestones alternating with calcareous shale interbeds. (a) Tight to isoclinal folds in the hangingwall of a small-scale reverse fault. Road cut, Praha-Radotín (near Cement plant), coordinates (WGS84 datum): 49.9968972° N, 14.3391594° E. (b) Disharmonic folding developed as a series of smaller-wavelength folds controlled by a thick limestone bed. Height of the outcrop *c*. 20 m. Budňany Rock in Karlštejn, coordinates (WGS84 datum): 49.9346564° N, 14.1809022° E. (c) Distant view on complexly folded limestone–shale succession. Height of the outcrop *c*. 15 m. Barrande's Rock, Praha-Malá Chuchle, coordinates (WGS84 datum): 50.0349111° N, 14.4019325° E. (d) Asymmetrical upright buckle folds. Barrande's Rock, Praha-Malá Chuchle, coordinates (WGS84 datum): 50.0349111° N, 14.4019325° E. (e) Close-up on accommodation structures (hinge thrusts, carinate hinges) that are commonly associated with the buckle folds. Barrande's Rock, Praha-Malá Chuchle, coordinates (WGS84 datum): 50.0349111° N, 14.4019325° E.

https://doi.org/10.1017/S0016756817000875 Published online by Cambridge University Press

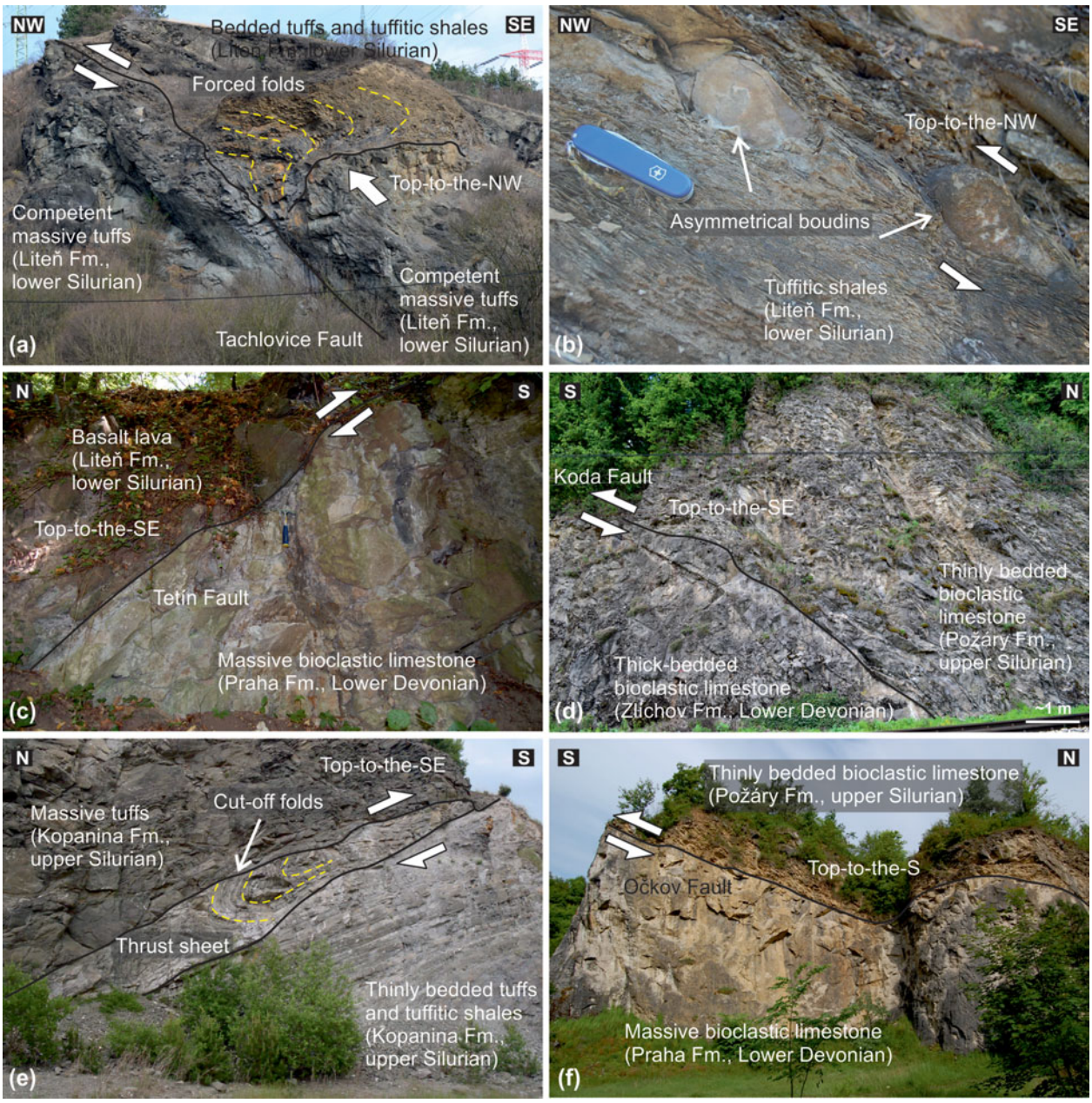

Figure 10. (Colour online) Examples of major reverse/thrust faults that cut the Prague Syncline. (a) The Tachlovice Fault (Set I) duplicates basaltic pyroclastic rocks and deforms the overlying bedded sequence into forced folds; note the folds and relative hangingwall displacement indicate top-to-the-NW tectonic transport (see also Horný, 1965). Height of the outcrop *c*. 30 m. Disused quarry ~580 m SW of Lištice near Beroun, coordinates (WGS84 datum): 49.9572917° N, 14.0968367° E. (b) Asymmetrically boudinaged competent bed within strongly sheared shales near the Tachlovice Fault indicating top-to-the-NW kinematics. Swiss Army penknife (9 cm long) for scale. Road cut Černidla ~1.8 km S of Loděnice, coordinates (WGS84 datum): 49.9809161° N, 14.1579681° E. (c) Close-up on the Tetín Fault. Hammer for scale is 33 cm long. Outcrop Šanův kout 1.1 km SSW of Hostim, coordinates (WGS84 datum): 49.9521106° N, 14.1228069° E. (d) Close-up on the Koda Fault. Railroad cut in Srbsko, coordinates (WGS84 datum): 49.9377411° N, 14.1309381° E. (e) Newly recognized Kosov Fault cutting across the Silurian volcanic rocks and indicating top-to-the-SE tectonic transport. Trees in the forefront are *c*. 3 m high. Disused quarry Kosov near Králův Dvůr; coordinates (WGS84 datum): 49.9377031° N, 14.0537014° E. (f) The Očkov Fault attributed to Set II faults with top-to-the-S hangingwall displacement. Height of the outcrop *c*. 15 m. Disused quarry Kobyla, 1.4 km SE of Koněprusy, coordinates (WGS84 datum): 49.9133644° N, 14.0813978° E.

virtually the same as in central Domain 1 (Figs 4, 6). In contrast, the southwestern closure (Domain 3) represents a deeper section exhumed in the footwall of a major ~NW–SE-trending normal fault cutting across the whole syncline (the Tobolka Fault in Figs 1b, 6). Thus, Domain 3 exposes mostly the Silurian to Lower Devonian part of the succession. Furthermore, the southeastern closure has a broad hinge and exhibits an internally complex dome-and-basin architecture (Fig. 2). The individual anticlines and synclines are elongated in an ~E–W direction (Figs 2, 4, 6), i.e. at an angle to the overall trend of the Prague Syncline. Bedding dips shallowly in most cases and is more variable in terms of strike (Fig. 6).

https://doi.org/10.1017/S0016756817000875 Published online by Cambridge University Press

Figure 11. (Colour online) Examples of small-scale low-angle duplexes, thrust faults and associated anticlines in the Silurian–Devonian core of the Prague Syncline. Note the duplexes and thrust faults exhibit variable orientations and kinematics. (a) A fault-propagation anticline in Lower Devonian limestones in the hangingwall of the Tetín Fault. Outcrop ~1.2 km S of Hostim, coordinates (WGS84 datum): 49.9499464° N, 14.1303481° E. (b) Duplexes indicating centimetre-scale bedding-parallel displacement. Disused quarry Mramorka ~880 m NNE of Chýnice, coordinates (WGS84 datum): 50.0037881° N, 14.2701194° E. (c) A small-scale anticline detached during bedding-parallel slip. In terms of orientation, the anticline corresponds to ~N–S shortening associated with younger phase (Set II) thrust faults. Outcrop 340 m NNE of Hostim, coordinates (WGS84 datum): 49.9636000° N, 14.1309717° E. (d, e) Small-scale duplexes indicating opposite kinematics on a single outcrop. Railroad cut in Praha-Zlíchov, coordinates (WGS84 datum): 50.0501233° N, 14.4054794° E. Swiss Army penknife (9 cm long) for scale.

4. Brittle deformation of the Prague Syncline

4.a. Reverse and thrust faults

The Prague Syncline is cross-cut by a number of faults (Figs 2, 4, 6) of various dimensions (ranging from basin-wide to metre-scale), amounts of displacement (which is difficult to constrain precisely), ages (ranging from early pre- and syn-sedimentary to post-Cretaceous) and kinematics (reverse, strike-slip, normal, oblique). The faults were commonly multiply reactived. Here we concentrate on reverse and thrust faults that are directly relevant to shortening of the basin and are geometrically and temporally related to the large-scale folds.

Several major reverse and thrust faults were documented mostly within the Silurian–Devonian core of the syncline and are more abundant in its south-eastern limb (Fig. 6). On the map, they extend for

https://doi.org/10.1017/S0016756817000875 Published online by Cambridge University Press

several kilometres or even tens of kilometres in length and their traces are roughly parallel to lithological contacts (Fig. 6). Importantly, the major reverse and thrust faults are doubly vergent with opposite dips and hangingwall transport directions in each limb of the Prague Syncline (Figs 5, 6). In outcrops, these major faults are expressed either as a single, sharp fault plane (Fig. 10) or comprise up to several metres thick zones of anastomosing smaller faults with associated fault breccia, well-developed pressure-solution cleavage and metre-scale folds. In addition, a number of minor, small-scale reverse and thrust faults were documented within the Silurian–Devonian succession; they are commonly associated with duplexes and fault-related folds (Fig. 11).

Analysis of map-scale relationships and fault planes, lineations (striations, calcite slickenfibres) and kinematic indicators in outcrops reveals two distinct sets of reverse and thrust faults in the Prague Syncline (referred to as Set I and II in this study). Set I contains faults with planes dipping either to the ~NW or ~SE at moderate angles and recording top-to-the-NW or top-to-the-SE kinematics, respectively. These faults occur mostly in Domain 1 (Fig. 6). The most significant large-scale examples of this set include the Tachlovice, Tetín, Koda and Kosov faults (Figs 6, 10a–e). Set II includes faults with planes dipping to the ~N to ~NNE at moderate to steep angles and associated with top-to-the-S kinematics (Figs 6, 10f); they occur mostly in the southeastern closure of the Prague Syncline (Domain 3; Figs 4, 6). A large-scale example of this set is the Očkov Fault (Figs 6, 10f), with a total displacement of *c.* 2.5 km (Röhlich, 2007). Reverse and thrust faults are rare in the opposite, northeastern closure of the syncline (Domain 2); we documented there only one tens-of-metres-scale SE-dipping fault with top-to-the-NE kinematics (Fig. 6).

A palaeostress estimation from the two main fault sets using the dihedra method (implemented in the TectonicsFP software; http://www.tectonicsfp.com) indicates that Set I formed in response to ~NW–SW subhorizontal compression (Fig. 12a; the maximum principal stress σ_1 trend and plunge are 305° and 07°, respectively) and nearly vertical minimum principal stress (σ_3; orientation is 172°/80°). Set II records a different stress field and formed in response to ~NNW–SSE subhorizontal compression (Fig. 12b; σ_1 orientation is 347°/13°, σ_3 orientation is 222°/69°).

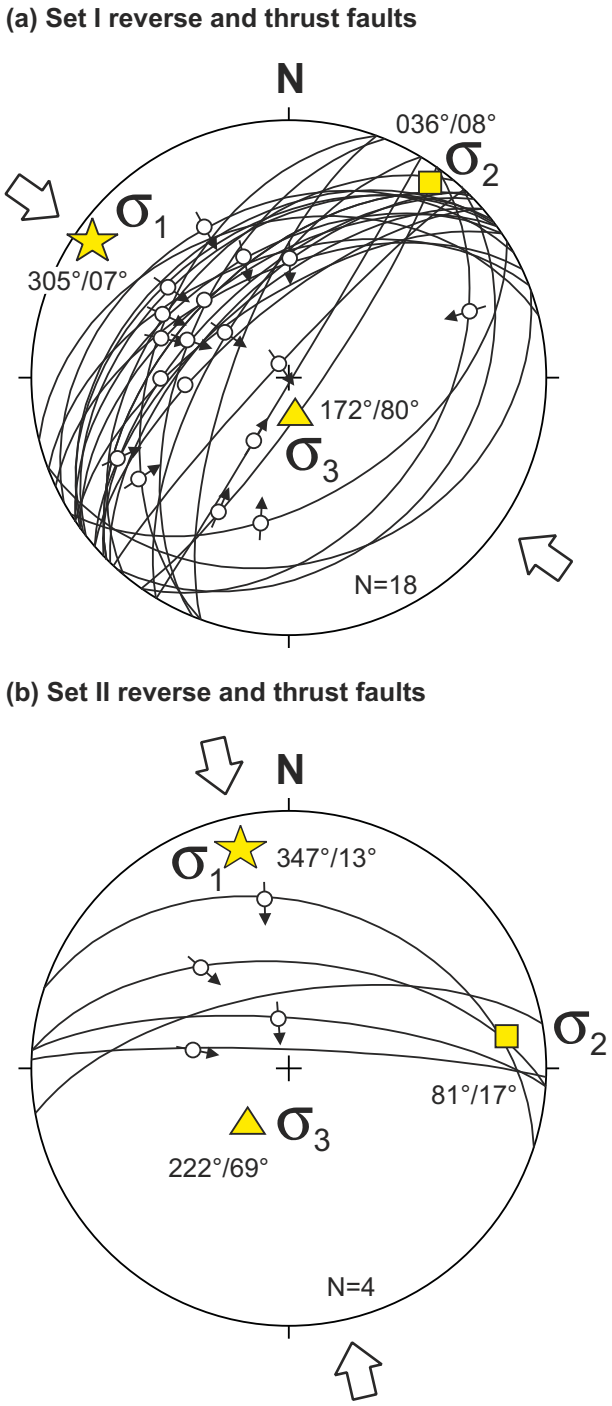

Figure 12. (Colour online) Fault-slip data for both major and minor reverse/thrust faults in the Prague Syncline. The data show two distinct populations of faults (Sets I and II), indicating two different palaeostress tensors.

4.b. Fold axis-perpendicular fractures

Systematic minor fractures observed in outcrops include mostly extension fractures (joints) and veins that form several, commonly reactivated sets that formed over a protracted 'life span' of the Prague Syncline. The earliest fractures are ~E–W neptunian dykes that developed already during deposition of the Lower Devonian reef limestones (Chlupáč, 1996). Several other fracture sets formed during the Variscan orogeny, and even younger fracturing events record post-Variscan intraplate deformation until Quaternary times. A thorough analysis of this polyphase history of brittle fracturing in the Prague Syncline is beyond the scope of this paper and will be presented elsewhere; here we briefly describe only one set particularly relevant to Variscan folding. Based on relative cross-cutting relationships, this set is one of the earliest to form and includes syntectonic subvertical ~NW–SE-striking fractures that are nearly perpendicular to the fold axes and strike of the bedding (Fig. 6). These

https://doi.org/10.1017/S0016756817000875 Published online by Cambridge University Press

fractures occur in most outcrops; they are either barren or filled by calcite to form several millimetres to centimetres thick veins. In all cases, they display macroscopically unrecognizable displacement along the fracture plane and none to small (millimetres to several centimetres for veins) displacement perpendicular to it; thus they formed as mode I (opening) extension fractures (joints).

5. Estimation of finite shortening of the Prague Syncline

The simple style of kilometre-wavelength folds, well-constrained stratigraphy and regionally continuous stratigraphical successions provide a suitable setting to estimate the finite shortening recorded by the Prague Syncline during Variscan plate convergence. The underlying assumptions are (1) plane-strain deformation, which is justified by the negligible syncline axis-parallel extension as evidenced by the extension fractures; (2) a low-temperature flexural-slip mechanism of folding, which is in concert with the observed fold characteristics and slickenfibres along bedding planes (Figs 8d, 9); and (3) no significant volume loss on a basin scale, which is in agreement with only locally developed small-scale stylolites and pressure-solution cleavage. Estimation of the minimum finite shortening was pursued in Domain 1 which records predominantly the ~NW–SE compression and is least overprinted by younger events (Figs 4, 6, 12).

Below we combine two approaches to estimate approximately the finite shortening in the syncline axis-perpendicular direction. The first approach uses the dip of tilted bedding in the regional monoclines (fold limbs). Dip of bedding relates to horizontal shortening ε_h of a bed of unit length as follows

$$\varepsilon_h = \frac{(L_0 - L_f)}{L_0} = 1 - cos\alpha \qquad (1)$$

where L_0 and L_f are the original and finite width of the deformed bed package and α is dip of bedding (e.g. Cao *et al.* 2015). Our structural data show that the bedding dip mostly ranges from 20° to 50° across the syncline and that there is no significant difference between stratigraphical units in both limbs and the core of the syncline (Figs 4, 5, 6, 13a). Exceptions are only a few locations where bedding has been steepened up to 60°–70° or even to almost vertical within smaller-scale folds (Fig. 9). The prevailing moderate bedding dips correspond to about 5–35 % horizontal shortening (Fig. 13a), which is also in agreement with values expected in chevron folds of comparable geometry (Ramsay, 1974).

Second, the idealized (unbalanced) cross-section in Figure 5 was restored with the assumption of constant length and thickness of the lithostratigraphical units before and after deformation and by removal of rigid-body translation along faults (e.g. Chamberlin, 1910; Dahlstrom, 1969; Groshong *et al.* 2012 and

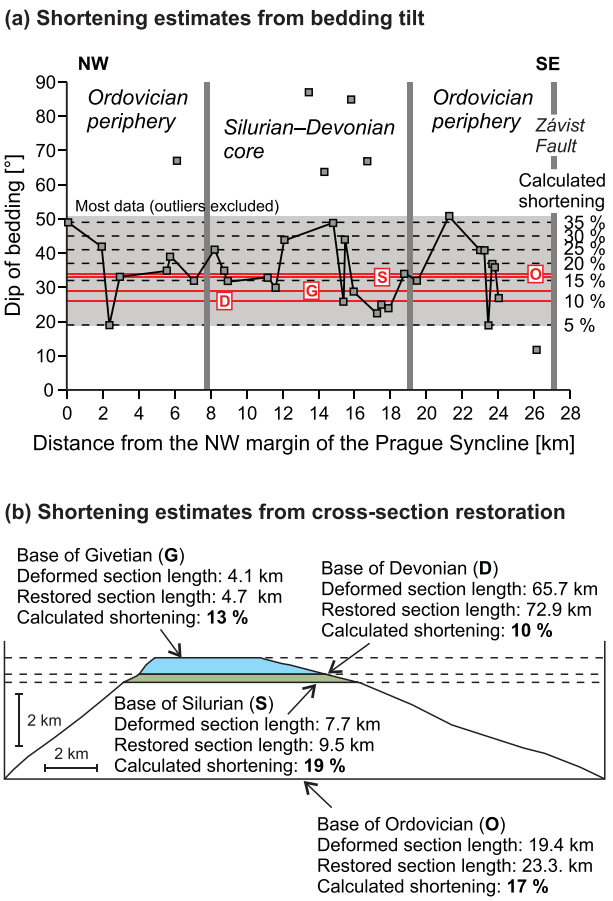

Figure 13. (Colour online) (a) Dip of bedding plotted against the distance from the NW margin of the Prague Syncline. The dip values mostly fall between 20° and 50° and correspond to *c.* 5–35 % shortening, respectively. (b) Restored cross-section A–A´from Figure 5. Base of the Ordovician is difficult to constrain and was estimated to parallel the Ordovician–Silurian boundary. The calculated values of finite shortening of the Prague Syncline range from 10 % to 19 % and fit well those estimated from dip of bedding (red lines in (a)).

references therein). It should be emphasized that this method provides only a crude minimum estimate of finite shortening recorded by the syncline, as the original lateral extent, and thus the initial across-strike length of the main stratigraphical units (Ordovician, Silurian and Devonian), is unknown owing to erosion and fault truncation (Figs 4, 5). The thickness of the individual units is well constrained from the geological map and cross-section along the syncline axis (Figs 4, 5) but remains unknown at its eroded and faulted margins. Despite these limitations, cross-section restoration indicates a range of 10–19 % of total shortening recorded by the Prague Syncline (Fig. 13b), which is in agreement with shortening estimation from bedding dips (Fig. 13a).

6. Structures recording late-stage thinning of the Prague Syncline

In some places, the earlier compressional structures have been overprinted by structures resulting from

https://doi.org/10.1017/S0016756817000875 Published online by Cambridge University Press

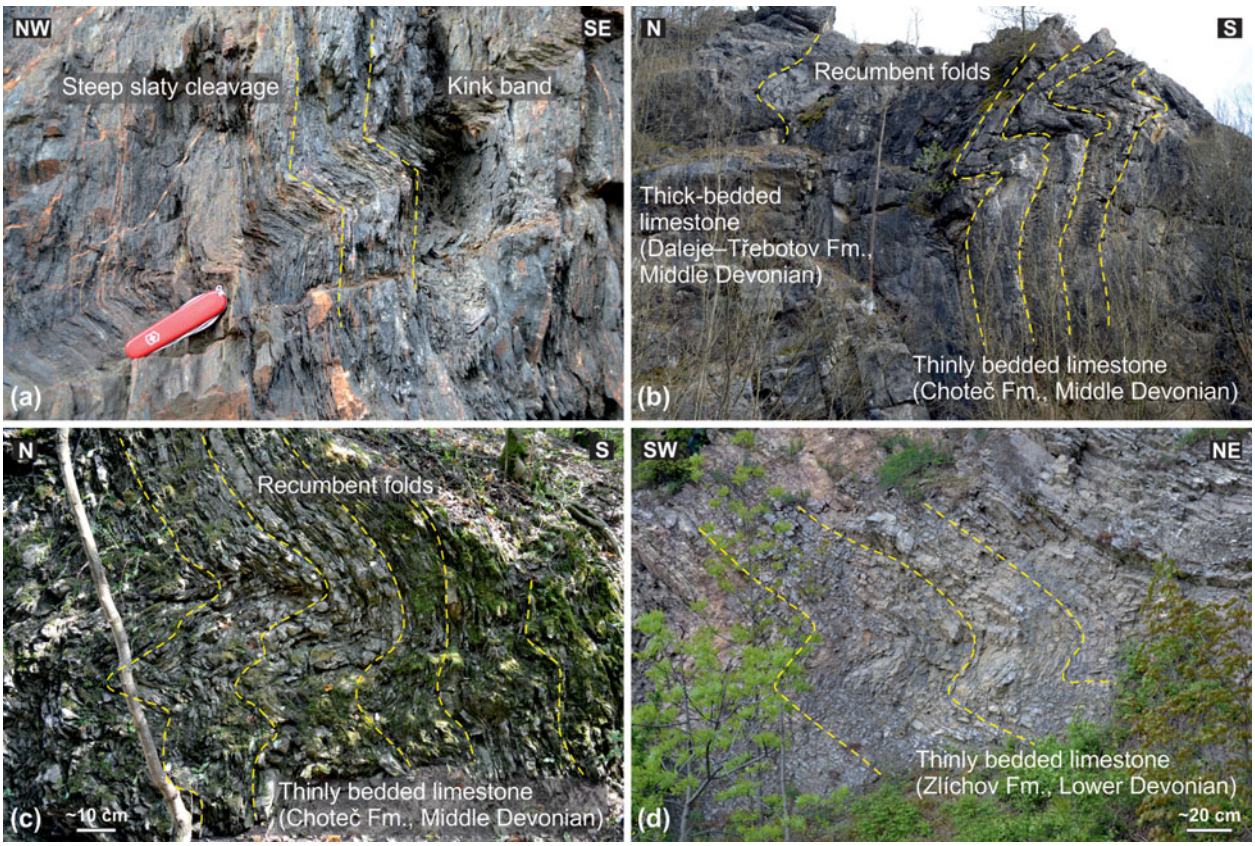

Figure 14. (Colour online) Deformational structures indicating localized vertical shortening of the Prague Syncline and its Cadomian basement. The shortening is superimposed on steep cleavage and folding of the syncline. (a) Monoclinal kink band overprinting Cadomian slaty cleavage (Blovice accretionary complex). Swiss Army penknife (9 cm long) for scale. Railroad cut 1.3 km SE of Nižbor, coordinates (WGS84 datum): 49.9979572° N, 14.0197431° E. (b) Devonian limestones steeply tilted during the main phase of ~NW–SE shortening and then overprinted by tight recumbent N-vergent folds during later vertical shortening. Height of the outcrop *c*. 10 m. Disused quarry Na Škrábku ~400 m NW of Choteč; coordinates (WGS84 datum): 49.9888628° N, 14.2789369° E. (c) Recumbent S-vergent folds in thinly bedded limestones. Disused quarry Hlubočepské jezírko, Praha-Hlubočepy, coordinates (WGS84 datum): 50.0415536° N, 14.3853844° E. (d) Recumbent NE-vergent folds in thinly bedded limestones. Praha-Zlíchov; coordinates (WGS84 datum): 50.0399969° N, 14.4043611° E.

vertical shortening (Fig. 14). For instance, monoclinal contractional kink bands frequently overprint subvertical cleavage in the Cadomian slates to the NW of the Prague Syncline (Fig. 14a). The kink band planes dip at moderate angles to the ~NW and have ~NE–SW-trending subhorizontal axes. Another example of these structures is metre-scale asymmetrical recumbent buckle folds superimposed on steeply dipping bedding in the Lower Devonian core of the Prague Syncline (Fig. 14b–d). Importantly, these folds occur in both limbs of the syncline away from any major thrust faults and exhibit opposite vergence. Together with minor bedding-parallel detachments and duplexes, they indicate inward tectonic transport (down-dip, symmetrical with respect to the syncline axis) during vertical shortening (Fig. 14b–d). This late-stage thinning of the syncline is also documented by several major ~NW–SE-trending normal faults and by exhumation of deeper stratigraphical levels (Domain 3) along the Tobolka Fault in the SW (Figs 4, 6).

7. Discussion

7.a. Large-scale architecture and structural evolution of the Prague Syncline

Our structural analysis corroborates that the Prague Syncline exhibits a simple architecture and fold style (Figs 4–6; e.g. Havlíček, 1963; Chlupáč *et al.* 1998; Röhlich, 2007), defined by outer, inward-dipping monoclines of the Ordovician siliciclastic rocks and by smaller-wavelength anticlines and synclines in the Silurian–Devonian core. Homogeneous strike of bedding across the syncline and no statistically significant difference in the bedding dip in the four lithomechanical units as defined above (Figs 4–6, 13a) suggest that the basin fill was folded as a more or less coherent multilayer. Orientation of bedding and of both major and outcrop-scale folds indicate that the earliest deformational phase was ~NW–SE horizontal principal shortening associated with fairly minor ~NE–SW horizontal principal extension along the syncline axis (Fig. 6). Field relationships suggest that this

https://doi.org/10.1017/S0016756817000875 Published online by Cambridge University Press

shortening was predominantly accommodated by buckle folds (Fig. 9) and by major reverse and thrust faults of Set I (Fig. 12a). These faults are geometrically and kinematically compatible with the large-scale folds and accommodated outward displacement of material in the opposite limbs of the syncline (Figs 5, 6, 10a–e). Unlike the major faults, the rare metre-scale duplexes and reverse/thrust faults show highly varied kinematics (Fig. 6), interpreted here as reflecting heterogeneous, small-displacement flow of material but still during the same ∼NW–SE overall shortening. Consequently, the syncline evolved into a doubly vergent compressional fan associated with thickening of the upper crust, achieved mainly by buckling and less so by reverse/thrust faulting (Fig. 5).

Our structural study has also revealed structures recording ∼N–S shortening at both ends of the Prague Syncline (Figs 6, 10f, 13b). The ∼N–S shortening was superposed onto ∼NE–SW-trending folds and is exemplified by the map-scale dome-and-basin architecture of the SW closure (Type 1 fold interference pattern of Ramsay, 2003; Figs 4, 6), small-scale buckle folds and contractional duplexes (Fig. 11a, c), and especially by Set II reverse/thrust faults (Figs 6, 10f, 13b). Furthermore, our unpublished U–Pb ages of calcite slickenfibres suggest that the Set II Očkov Fault (Fig. 10f) initiated during Middle Triassic (Anisian/Ladinian) times at *c.* 242 Ma and was reactivated during Late Cretaceous (Cenomanian) times at *c.* 99 Ma. We interpret this polyphase faulting activity to record intraplate stresses generated by far-field plate convergence in the Alpine realm.

Lastly, we interpret kink bands, recumbent folds and normal faults (Section 6; Fig. 14) in terms of vertical shortening and collapse of the previously thickened upper crust. These processes can be well correlated with normal displacement along crustal-scale shear zones (with a minimum throw of 10 km) that juxtaposed the upper-crustal Teplá–Barrandian Unit against the deep middle and lower crust (Moldanubian Unit; Fig. 1b; Zulauf, 1994; Zulauf *et al.* 2002; Dörr & Zulauf, 2010). The ductile phase of the upper-crustal collapse was previously constrained to *c.* 346–337 Ma, with the main exhumation event in the Moldanubian footwall dated at *c.* 340–339 Ma (Žák, Holub & Verner, 2005; Dörr & Zulauf, 2010; Žák *et al.* 2012; Žák, Sláma & Burjak, 2017; Kubínová *et al.* 2017).

It should be noted that the above proposed structural interpretation is different from a nappe hypothesis for Variscan shortening of the Prague Syncline (e.g. Melichar, 2004 and a number of conference abstracts). In this hypothesis, which tested an end-member case and triggered vigorous scientific discussion, the syncline was interpreted as a stack of allochthonous nappes transported from the NW to SE and subsequently folded into a 'synform'. We emphasize that the latter term is appropriate for metamorphic complexes with unknown younging direction, but not for a sedimentary succession where the overall upward younging has been recognized as early as the 1850s (Barrande, 1852) and elaborated using high-resolution stratigraphy over the last decades (e.g. Chlupáč, 1988; Hladíková, Hladil & Kříbek, 1997; Crick *et al.* 2001; Frýda, Hladil & Vokurka, 2002; Buggisch & Mann, 2004; Slavík, 2004; Koptíková *et al.* 2010; Hladil *et al.* 2011; Vacek, 2011; Slavík *et al.* 2012; Da Silva *et al.* 2016; Weinerová *et al.* 2017). The nappe hypothesis implies that the reverse/thrust faults observed in the NW limb of the syncline (e.g. Tachlovice Fault in Fig. 6) should have originated as flat or low-angle detachments with top-to-the-SE kinematics, and after folding and steepening of the fault planes they should appear as normal faults. These faults should also connect with those cropping out at different stratigraphical levels (owing to their presumed flat-ramp geometry) in the opposite, SE limb of the syncline.

There are a number of arguments against this hypothesis (see also Röhlich, 2007 for discussion). (1) The root zone, where these nappes were derived from, is yet to be found. (2) The location and presumed linkage of faults at depth is not supported by any subsurface data such as boreholes or seismic sections. (3) The presumed major detachments are not exposed along their entire length and some have never been observed (e.g. the 'main detachment' at the Ordovician–Silurian boundary shown in fig. 1 of Slobodník *et al.* 2012). Large portions of the faults are concealed and thus it remains unclear whether they are connected at all. (4) Kinematics documented on the major reverse/thrust faults is opposite in each limb of the syncline (Figs 5, 6, 10). This is exemplified by the Tachlovice and Koda faults (Figs 6, 10a, b, d). (5) Kinematics on metre-scale structures (e.g. duplexes, fault-propagation folds) is variable (Fig. 6), displacement negligible and they rather reflect bedding-parallel slip or local outflow of material during folding. Importantly, their exact temporal relationship to the major faults is unknown. Some of these structures were shown poorly located or in a not fully accurate orientation in Melichar (2004) (compare, e.g., fig. 6c with our Fig. 11c). (6) Minor structures indicating normal (down-dip) bedding-parallel displacement occur in both limbs of the Prague Syncline (Fig. 14), show an opposite vergence and record its late-stage vertical shortening (thinning). (7) The amount of displacement along the reverse/thrust faults as apparent from the map and stratigraphical relationships is significantly less than required for nappes, or it cannot be constrained quantitatively. Note that the net slip along a fault can be rigorously evaluated only if it displaces an originally continuous structural line. Using diverse facies juxtaposed by faulting is not reliable given their unknown original extent, likely modification by syn-sedimentary tectonics and unclear relative position before Variscan faulting. (8) Furthermore, the presumed flat-and-ramp geometry inferred for the Tachlovice Fault from the stratigraphical separation diagrams (Knížek, Melichar & Janečka, 2010) may be equally explained by variable displacements along shorter transverse faults during folding. A number of

https://doi.org/10.1017/S0016756817000875 Published online by Cambridge University Press

such faults cut the Tachlovice Fault at a high angle (Fig. 2) but were omitted in maps and stratigraphical separation diagrams in Knížek, Melichar & Janečka (2010). (9) Finally, we have shown that the thrusting was polyphase (Figs 10, 12) and likely involved post-Variscan, Mesozoic shortening (e.g. the Očkov Fault).

7.b. Crustal deformation and plateau uplift in the Variscan orogen

As pointed out in the Introduction, one of the outstanding issues that has been debated and still remains poorly understood is the evolution of palaeotopography in the Variscan belt from the Late Devonian convergence to the end-Carboniferous termination of orogenic processes. Analysis of Variscan deformation of the Prague Basin, sitting on top of the presumed orogenic plateau, may add some new points to this debate. We argue that a key aspect in the interpretation of palaeoelevation gradients is a detailed three-dimensional characterization of Variscan deformation of the orogenic upper crust. We have shown that the Prague Syncline was vertically thickened and horizontally shortened by *c.* 10–19 % (Fig. 13) but records a significantly smaller amount of horizontal stretching, perhaps as little as a few per cent. These estimates are in agreement with finite strain analysis on conglomerates in the Cadomian basement along the southeastern faulted margin of the Prague Syncline (Rajlich, Schulmann & Synek, 1988). These inferences are further supported by the existing apatite fission-track ages, which suggest maximum burial, and thus crustal thickening, in the Prague Syncline and vicinity during Late Devonian to early Carboniferous times (Glasmacher, Mann & Wagner, 2002; Filip & Suchý, 2004; Suchý *et al.* 2007). Moreover, *c.* 1.5–3 km of overlying sediments that have been removed by erosion must be added to this thickened 'crustal column'. In summary, the structural inventory of the Prague Basin indicates build-up of significant palaeoelevation during the Variscan orogeny (Fig. 15a, b; see Dörr & Zulauf, 2010 for discussion).

Despite the absolute reference frame and the exact amount of eroded material being unknown, we may expand on the above inferences by assuming that palaeoelevation was closely related to the three-dimensional deformation of the upper crust. Then, a synthesis of the existing structural data from the Teplá–Barrandian Unit suggests that it was not simply an uplifted and thoroughly flat surface. Hajná *et al.* (2012) and Tomek, Žák & Chadima (2015) demonstrated that the Teplá–Barrandian Unit recorded a fairly uniform ∼NW–SE to ∼WNW–ESE shortening during Variscan convergence but they also identified several ∼NE–SW-trending zones of lateral (orogen-parallel) extrusion. Although the precise radiometric ages are still scarce, the existing data indicate that the main shortening affected not only the upper crust but also deeper levels (greenschist-facies rocks exposed in the west and southwest; Zulauf, 1997, 2001) and progressed from *c.* 380–360 Ma in the NW to *c.* 360–350 Ma in the SE (Dörr & Zulauf, 2010; Hajná *et al.* 2012). We thus suggest that the palaeoelevation within this upper plate varied and reflected a spatially varying horizontal stretching to vertical thickening ratio (S/T). We envision the differentiated within-plateau palaeotopography as ∼NE–SW-trending elevations, where local thickening dominates, alternating with topographic depressions over lateral extrusion zones (Fig. 15b). As greatly exemplified by the Prague Basin, tectonic inheritance may have controlled the loci of crustal thickening or lateral extrusion. The previously thinned crust of the Prague Basin was a precursor for thickening whereas some of the segments of the Cadomian crust may have acted as rigid backstops driving lateral extrusion (Fig. 15b). Were the above inferences correct, the Teplá–Barrandian Unit may serve as an instructive ancient example of complex three-dimensional deformations associated with uplift and lateral extrusion of orogenic plateaus, as predicted, for instance, by the analogue and numerical modelling of Cruden, Nasseri & Pysklywec (2006) and Bajolet *et al.* (2015) and documented in the recent Tibet (e.g. Royden *et al.* 1997; Yin & Harrison, 2000; DeCelles, Robinson & Zandt, 2002; Andronicos, Velasco & Hurtado, 2007; Li *et al.* 2015), Puna–Altiplano (e.g. Riller & Oncken, 2003) and Turkish–Iranian plateau (e.g. Copley & Jackson, 2006; Mouthereau, Lacombe & Vergés, 2012).

7.c. Mechanisms of destruction of the Variscan orogenic plateau

Unlike the still active, modern orogenic plateaus, the Variscan example allows completing the story to its end. The structural and geochronological studies suggest that the 'Bohemian' plateau was supported for several tens of millions of years (*c.* 380–346 Ma) by the syn-convergent compression (Fig. 15a, b) but then rapidly collapsed at *c.* 346–338 Ma (Fig. 15c). Structures indicating a switch to vertical shortening in the Prague Syncline and its Cadomian basement may record this collapse stage (Fig. 14). The outstanding question thus arises: what was the trigger for such rapid collapse and destruction of the high topography? For instance, Dörr & Zulauf (2010) invoked delamination of lithospheric mantle (Fig. 15c) whereby inflow of new hot mantle caused thermal weakening and abrupt rheological failure of the lower crust beneath the plateau. Nevertheless, our inferences developed above suggest that there may have been other additional processes that contributed to the destruction of the orogenic plateau.

Firstly, the southeastern margin of the Teplá–Barrandian plateau along its entire length was intruded by voluminous granodioritic arc plutons at *c.* 346 Ma (Fig. 15c). Hence, it may be assumed that this hinterland-facing plateau margin lost much of its strength owing to thermal softening and lubrication

https://doi.org/10.1017/S0016756817000875 Published online by Cambridge University Press

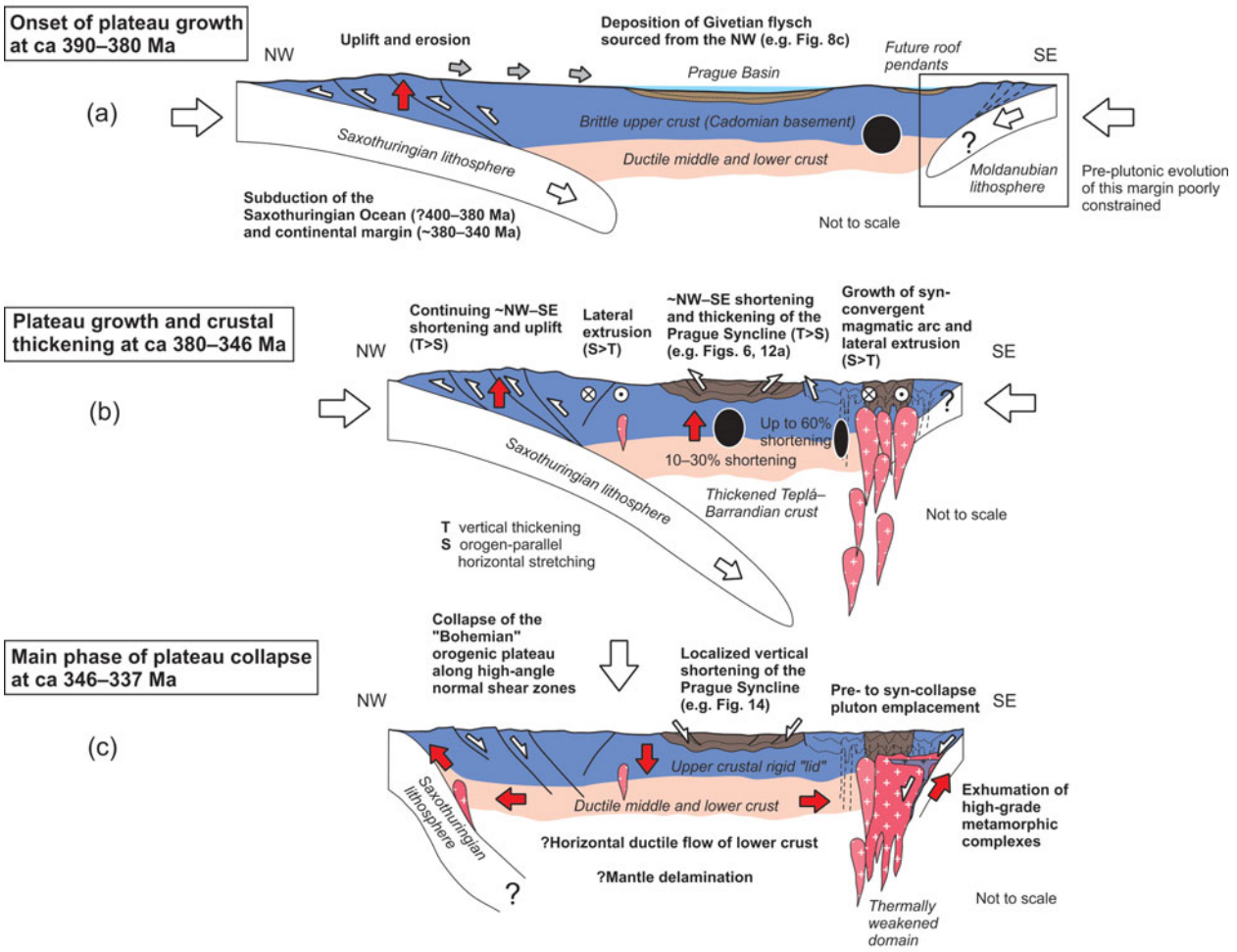

Figure 15. (Colour online) (a, b) A tectonic model for the growth and (c) collapse of an orogenic plateau in the Bohemian Massif. The model builds on new structural data and interpretations from the Prague Syncline (this study) and previous models published in Zulauf (1994), Zulauf *et al*. (2002), Žák, Holub & Verner (2005), Dörr & Zulauf (2010), Hajná *et al*. (2012) and Žák *et al*. (2012). See text for discussion.

by magmas (e.g. Hollister & Crawford, 1986; Pavlis, 1996; Dörr & Zulauf, 2010).

Secondly, the plateau collapse temporally overlaps with movement along the intracontinental, WNW–ESE-trending dextral strike-slip faults from *c.* 345 Ma onwards (e.g. Aleksandrowski *et al.* 1997; Mazur & Aleksandrowski, 2001; Mazur *et al.* 2006; Hofmann *et al.* 2009; Verner *et al.* 2009; Pertoldová *et al.* 2010; Hajná *et al.* 2012). Indeed, Arthaud & Matte (1977), Badham (1982), Matte (1986, 2001), Lewandowski (2003) and Martínez Catalán (2011, 2012) proposed that the whole Variscan belt switched from a frontal convergence mode to overall dextral strike-slip between Gondwana and Laurussia at *c.* 345 Ma, leading to major reorientation in the tectonic forces shaping the orogen. The NW–SE-trending normal faults that accommodated exhumation of various structural levels of the Prague Syncline (Fig. 6) suggest such stress reorientation and increased amount of NE–SW stretching, which is kinematically compatible with the expected crustal strain orientations during the far-field dextral strike-slip. This interpretation is also consistent with numerical modelling by Henk (1999), who proposed that gravitational forces alone are insufficient to cause the collapse of the Variscan orogen and advocated a key role of far-field tectonic forces.

8. Conclusions

(1) The Prague Syncline exhibits a simple structure, defined by buckle folds of up to several kilometres wavelength cross-cut by major reverse/thrust faults, both recording horizontal ~NW–SE shortening and coeval ~NE–SW extension. Owing to this deformation, the syncline evolved into a doubly vergent compressional fan associated with significant crustal thickening. Similar compressional structures are also observed in the deeper structural levels exposed to the southwest of the Prague Basin. Subsequently, these Late Devonian/early Carboniferous structures were overprinted by vertical shortening accommodated by localized recumbent folds and normal faults. This deformation event can be correlated with normal displacement along ductile shear zones that juxtaposed the Teplá–Barrandian upper crust against the deep middle and lower crust (Moldanubian Unit) at *c.* 346–337 Ma.

https://doi.org/10.1017/S0016756817000875 Published online by Cambridge University Press

(2) Even younger is a newly recognized deformation phase represented by ~N–S shortening affecting both ends of the syncline. The above documented deformational sequence and stratigraphical relationships exclude a previous interpretation of the Prague Syncline as a stack of allochthonous SE-directed nappes folded together into a 'synform'.

(3) The Prague Syncline records *c.* 10–19 % shortening and only minor syncline axis-parallel extension, implying significant vertical thickening and thus palaeoelevation of the Teplá–Barrandian upper crust during Variscan microplate convergence. A synthesis of finite deformation components and orientations across the Teplá–Barrandian Unit suggests a differentiated within-plateau palaeotopography with ~NE–SW-trending elevations, where local thickening dominates, alternating with topographic depressions over lateral extrusion zones. The loci of crustal thickening or lateral extrusion may have been controlled by tectonic inheritance.

(4) The Prague Syncline example may thus provide some new insights into a lifetime of Tibetan-type orogenic plateaus in other orogens: their growth may likely involve complex, progressive three-dimensional internal deformations of the overriding plate, with strain partitioning and development of alternating zones of thickening and lateral extrusion controlled by tectonic inheritance. Similarly, we argue for multiple interlinked processes contributing to plateau collapse in addition to gravity, including mantle delamination, voluminous magma emplacement and thermal softening in the hinterland, and far-field plate-boundary forces governed by changes in plate motions.

Acknowledgements. This paper is dedicated to the memory of Professor Ivo Chlupáč (1931–2002), a brilliant palaeontologist and geologist who devoted his entire professional career to research into the 'Barrandian' and promoted it to one of the world's classic areas of Lower Palaeozoic stratigraphy. We gratefully acknowledge Gernold Zulauf, Stanislaw Mazur and one anonymous reviewer for their constructive comments which helped to improve the original manuscript significantly. We also thank Olivier Lacombe for careful editorial handling and Jaroslava Hajná, Václav Kachlík, Filip Tomek, Petr Kraft and Wolfgang Dörr for discussions of various aspects of geology of the 'Barrandian'. Jaroslava Hajná and Filip Tomek also kindly provided maps that were modified in Figure 1. Pivovar Hostomice pod Brdy is highly appreciated for support and hospitality during fieldwork. This study was supported by project DKRVO 2013/03–2017/03 (National Museum, 00023272) of the Ministry of Culture, by the Czech Science Foundation through Grant No. 16–11500S (to Jiří Žák), and by the Charles University project PROGRES Q45.

References

Aifa, T., Pruner, P., Chadima, M. & Štorch, P. 2007. Structural evolution of the Prague synform (Czech Republic) during Silurian times: an AMS, rock magnetism, and paleomagnetic study of the Svatý Jan pod Skalou dikes. Consequences for the nappes emplacement. *Geological Society of America Special Paper* **423**, 249–65.

Aleksandrowski, P., Kryza, R., Mazur, S. & Zaba, J. 1997. Kinematic data on major Variscan strike-slip faults and shear zones in the Polish Sudetes, northeast Bohemian Massif. *Geological Magazine* **134**, 727–39.

Andronicos, C. L., Velasco, A. A. & Hurtado, J. M. 2007. Large-scale deformation in the India–Asia collision constrained by earthquakes and topography. *Terra Nova* **19**, 105–19.

Arthaud, F. & Matte, P. 1977. Late Paleozoic strike-slip faulting in southern Europe and northern Africa: result of a right-lateral shear zone between the Appalachians and the Urals. *Geological Society of America Bulletin* **88**, 1305–20.

Badham, J. P. N. 1982. Strike-slip orogens: an explanation for the Hercynides. *Journal of the Geological Society, London* **139**, 493–504.

Bajolet, F., Chardon, D., Martinod, J., Gapais, D. & Kermarrec, J. J. 2015. Synconvergence flow inside and at the margin of orogenic plateaus: lithospheric-scale experimental approach. *Journal of Geophysical Research* **120**, 6634–57.

Barrande, J. 1852. *Système Silurien du centre de la Bohême, 1ère Partie: Recherches Paléontologiques, Vol. 1, Planches. Crustacés: Trilobites*. Prague, Paris, 935 pp.

Beaumont, C., Hamilton, J. & Fullsack, P. 1996. Mechanical model for subduction–collision tectonics of Alpine-type compressional orogens. *Geology* **24**, 675–8.

Beaumont, C., Jamieson, R. A. & Nguyen, M. 2010. Models of large, hot orogens containing a collage of reworked and accreted terranes. *Canadian Journal of Earth Sciences* **47**, 485–515.

Beaumont, C., Jamieson, R. A., Nguyen, M. H. & Lee, B. 2001. Himalayan tectonics explained by extrusion of a low-viscosity crustal channel coupled to focused surface denudation. *Nature* **414**, 738–42.

Becq-Giraudon, J. F., Montenat, C. & Van Den Driessche, J. 1996. Hercynian high-altitude phenomena in the French Massif Central: tectonic implications. *Palaeogeography, Palaeoclimatology, Palaeoecology* **122**, 227–41.

Brenchley, P. J. & Štorch, P. 1989. Environmental changes in the Hirnantian (upper Ordovician) of the Prague Basin, Czechoslovakia. *Geological Journal* **24**, 165–81.

Buggisch, W. & Mann, U. 2004. Carbon isotope stratigraphy of Lochkovian to Eifelian limestones from the Devonian of central and southern Europe. *International Journal of Earth Sciences* **93**, 521–41.

Cao, W., Paterson, S. R., Memeti, V., Mundil, R., Anderson, J. L. & Schmidt, K. 2015. Tracking paleodeformation fields in the Mesozoic central Sierra Nevada arc: implications for intra-arc cyclic deformation and arc tempos. *Lithosphere* **7**, 296–320.

Chamberlin, R. T. 1910. The Appalachian folds of central Pennsylvania. *Journal of Geology* **18**, 228–51.

Chlupáč, I. 1988. Possible global events and the stratigraphy of the Palaeozoic of the Barrandian (Cambrian–Middle Devonian, Czechoslovakia). *Journal of Geological Sciences, Geology* **43**, 83–146.

Chlupáč, I. 1993. *Geology of the Barrandian: A Field Trip Guide*. Frankfurt am Main: Waldemar Kramer, 163 pp.

Chlupáč, I. 1996. Neptunian dykes in the Koněprusy Devonian: geological and palaeontological observations. *Bulletin of the Czech Geological Survey* **71**, 193–208.

Chlupáč, I. 2003. Comments on facies development and stratigraphy of the Devonian, Barrandian area, Czech Republic. *Bulletin of Geosciences* **78**, 299–312.

Chlupáč, I., Havlíček, V., Kříž, J., Kukal, Z. & Štorch, P. 1998. *Palaeozoic of the Barrandian (Cambrian to Devonian)*. Czech Geological Survey, 183 pp.

Copley, A. & Jackson, J. 2006. Active tectonics of the Turkish–Iranian Plateau. *Tectonics* **25**, TC6006. doi: 10.1029/2005TC001906.

Crick, R. E., Ellwood, B. B., Hladil, J., El Hassani, A., Hrouda, F. & Chlupáč, I. 2001. Magnetostratigraphy susceptibility of the Přídolian–Lochkovian (Silurian–Devonian) GSSP (Klonk, Czech Republic) and a coeval sequence in Anti-Atlas Morocco. *Palaeogeography, Palaeoclimatology, Palaeoecology* **167**, 73–100.

Cruden, A. R., Nasseri, M. H. B. & Pysklywec, R. 2006. Surface topography and internal strain variation in wide hot orogens from three-dimensional analogue and two-dimensional numerical vice models. In *Analogue and Numerical Modelling of Crustal-Scale Processes* (eds S. J. H. Buiter & G. Schreurs), pp. 79–104. Geological Society of London, Special Publication no. 253.

Culshaw, N. G., Beaumont, C. & Jamieson, R. A. 2006. The orogenic superstructure–infrastructure concept: revisited, quantified, and revived. *Geology* **34**, 733–6.

Dahlstrom, C. D. A. 1969. Balanced cross sections. *Canadian Journal of Earth Sciences* **6**, 743–57.

Dallmeyer, R. D. & Urban, M. 1994. Variscan vs. Cadomian tectonothermal evolution within the Teplá–Barrandian zone, Bohemian Massif, Czech Republic: evidence from $^{40}Ar/^{39}Ar$ mineral and whole-rock slate/phyllite ages. *Journal of the Czech Geological Society* **39**, 21–2.

Dallmeyer, R. D. & Urban, M. 1998. Variscan vs Cadomian tectonothermal activity in northwestern sectors of the Teplá–Barrandian zone, Czech Republic: constraints from $^{40}Ar/^{39}Ar$ ages. *Geologische Rundschau* **87**, 94–106.

Da Silva, A. C., Hladil, J., Chadimová, L., Slavík, L., Hilgen, F. J., Bábek, O. & Dekkers, M. J. 2016. Refining the Early Devonian time scale using Milankovitch cyclicity in Lochkovian–Pragian sediments (Prague Synform, Czech Republic). *Earth and Planetary Science Letters* **455**, 125–39.

DeCelles, P. G., Robinson, D. M. & Zandt, G. 2002. Implications of shortening in the Himalayan fold–thrust belt for uplift of the Tibetan Plateau. *Tectonics* **21**, 1062. doi: 10.1029/2001TC001322.

de Sitter, L. U. & Zwart, H. J. 1960. Tectonic development in supra and infra-structures of a mountain chain. In *Proceedings of the 21st International Geological Congress*, Copenhagen, pp. 248–56.

Dörr, W. & Zulauf, G. 2010. Elevator tectonics and orogenic collapse of a Tibetan-style plateau in the European Variscides: the role of the Bohemian shear zone. *International Journal of Earth Sciences* **99**, 299–325.

Dörr, W. & Zulauf, G. 2012. Reply to W. Franke on W. Dörr and G. Zulauf elevator tectonics and orogenic collapse of a Tibetan-style plateau in the European Variscides: the role of the Bohemian shear zone. *International Journal of Earth Sciences* **101**, 2035–41.

Dörr, W., Zulauf, G., Fiala, J., Franke, W. & Vejnar, Z. 2002. Neoproterozoic to Early Cambrian history of an active plate margin in the Teplá–Barrandian unit: a correlation of U–Pb isotopic-dilution-TIMS ages (Bohemia, Czech Republic). *Tectonophysics* **352**, 65–85.

Drost, K., Gerdes, A., Jeffries, T., Linnemann, U. & Storey, C. 2011. Provenance of Neoproterozoic and early Paleozoic siliciclastic rocks of the Teplá–Barrandian unit (Bohemian Massif): evidence from U–Pb detrital zircon ages. *Gondwana Research* **19**, 213–31.

Drost, K., Linnemann, U., McNaughton, N., Fatka, O., Kraft, P., Gehmlich, M., Tonk, C. & Marek, J. 2004. New data on the Neoproterozoic–Cambrian geotectonic setting of the Teplá–Barrandian volcano-sedimentary successions: geochemistry, U–Pb zircon ages, and provenance (Bohemian Massif, Czech Republic). *International Journal of Earth Sciences* **93**, 742–57.

Fatka, O., Kraft, J., Kraft, P., Mergl, M., Mikuláš, R. & Štorch, P. 1995. Ordovician of the Prague Basin: stratigraphy and development. In *Ordovician Odyssey: Short Papers for the 7th International Symposium on the Ordovician System* (eds J. D. Cooper, M. L. Droser & S. C. Finney), pp. 241–4. Las Vegas: The Pacific Section Society for Sedimentary Geology.

Fatka, O. & Mergl, M. 2009. The 'microcontinent' Perunica: status and story 15 years after conception. In *Early Palaeozoic Peri-Gondwana Terranes: New Insights from Tectonics and Biogeography* (ed. M. G. Bassett), pp. 65–101. Geological Society of London, Special Publication no. 325.

Ferrová, L., Frýda, J. & Lukeš, P. 2012. High-resolution tentaculite biostratigraphy and facies development across the Early Devonian Daleje Event in the Barrandian (Bohemia): implications for global Emsian stratigraphy. *Bulletin of Geosciences* **87**, 587–624.

Filip, J. & Suchý, V. 2004. Thermal and tectonic history of the Barrandian Lower Paleozoic, Czech Republic: is there a fission-track evidence for Carboniferous–Permian overburden and pre-Westphalian alpinotype thrusting? *Bulletin of Geosciences* **79**, 107–12.

Franěk, J., Schulmann, K., Lexa, O., Tomek, Č. & Edel, J. B. 2011. Model of syn-convergent extrusion of orogenic lower crust in the core of the Variscan belt: implications for exhumation of high-pressure rocks in large hot orogens. *Journal of Metamorphic Geology* **29**, 53–78.

Franke, W. 2006. The Variscan orogen in Central Europe: construction and collapse. In *European Lithosphere Dynamics* (eds D. G. Gee & R. A. Stephenson), pp. 333–43. Geological Society of London, Memoir no. 32.

Franke, W. 2012. Comment on Dörr and Zulauf: elevator tectonics and orogenic collapse of a Tibetan-style plateau in the European Variscides: the role of the Bohemian shear zone. Int J Earth Sci (Geol Rundsch) (2010) 99: 299–325. *International Journal of Earth Sciences* **101**, 2027–34.

Franke, W. 2014. Topography of the Variscan orogen in Europe: failed–not collapsed. *International Journal of Earth Sciences* **103**, 1471–99.

Frýda, J. & Frýdová, B. 2014. First evidence for the Homerian (late Wenlock, Silurian) positive carbon isotope excursion from peri-Gondwana: new data from the Barrandian (Perunica). *Bulletin of Geosciences* **89**, 617–34.

Frýda, J., Hladil, J. & Vokurka, K. 2002. Seawater strontium isotope curve at the Silurian/Devonian boundary: a study of the global Silurian/Devonian boundary stratotype. *Geobios* **35**, 21–8.

Glasmacher, U. A., Mann, U. & Wagner, G. A. 2002. Thermotectonic evolution of the Barrandian, Czech Republic, as revealed by apatite fission-track analysis. *Tectonophysics* **359**, 381–402.

Glodny, J., Grauert, B., Fiala, J., Vejnar, Z. & Krohe, A. 1998. Metapegmatites in the western Bohemian massif: ages of crystallisation and metamorphic overprint, as constrained by U–Pb zircon, monazite, garnet, columbite and Rb–Sr muscovite data. *Geologische Rundschau* **87**, 124–34.

Graveleau, F., Malavieille, J. & Dominguez, S. 2012. Experimental modelling of orogenic wedges: a review. *Tectonophysics* 538–540, 1–66.

Groshong, R. H., Bond, C., Gibbs, A., Ratliff, R. & Wiltschko, D. V. 2012. Preface: Structural balancing at the start of the 21st century: 100 years since Chamberlin. *Journal of Structural Geology* **41**, 1–5.

Hajná, J., Žák, J. & Kachlík, V. 2011. Structure and stratigraphy of the Teplá–Barrandian Neoproterozoic, Bohemian Massif: a new plate-tectonic reinterpretation. *Gondwana Research* **19**, 495–508.

Hajná, J., Žák, J. & Dörr, W. 2017. Time scales and mechanisms of growth of active margins of Gondwana: a model based on detrital zircon ages from the Neoproterozoic to Cambrian Blovice accretionary complex, Bohemian Massif. *Gondwana Research* **42**, 63–83.

Hajná, J., Žák, J., Kachlík, V. & Chadima, M. 2010. Subduction-driven shortening and differential exhumation in a Cadomian accretionary wedge: the Teplá–Barrandian unit, Bohemian Massif. *Precambrian Research* **176**, 27–45.

Hajná, J., Žák, J., Kachlík, V. & Chadima, M. 2012. Deciphering the Variscan tectonothermal overprint and deformation partitioning in the Cadomian basement of the Teplá–Barrandian unit, Bohemian Massif. *International Journal of Earth Sciences* **101**, 1855–73.

Halavínová, M., Melichar, R. & Slobodník, M. 2008. Hydrothermal veins linked with the Variscan structure of the Prague Synform (Barrandien, Czech Republic): resolving fluid–wall rock interaction. *Geological Quarterly* **52**, 309–20.

Havlíček, V. 1963. Tectogenetic disruption of the Barrandian Paleozoic. *Journal of Geological Sciences, Geology* **1**, 77–102.

Havlíček, V. 1980. Development of Paleozoic basins in the Bohemian Massif (Cambrian–Lower Carboniferous). *Journal of Geological Sciences, Geology* **34**, 31–65.

Havlíček, V. 1981. Development of a linear sedimentary depression exemplified by the Prague Basin (Ordovician–Middle Devonian; Barrandian area – central Bohemia). *Journal of Geological Sciences, Geology* **35**, 7–48.

Havlíček, V. 1982. Ordovician of Bohemia: development of the Prague Basin and its benthic communities. *Journal of Geological Sciences, Geology* **37**, 103–36.

Henk, A. 1999. Did the Variscides collapse or were they torn apart?: A quantitative evaluation of the driving forces for postconvergent extension in central Europe. *Tectonics* **18**, 774–92.

Hladíková, J., Hladil, J. & Kříbek, B. 1997. Carbon and oxygen isotope record across Pridoli to Givetian stage boundaries in the Barrandian basin (Czech Republic). *Palaeogeography, Palaeoclimatology, Palaeoecology* **132**, 225–41.

Hladil, J., Slavík, L., Vondra, M., Koptíková, L., Čejchan, P., Schnabl, P., Adamovič, J., Vacek, F., Vích, R., Lisá, L. & Lisý, P. 2011. Pragian–Emsian successions in Uzbekistan and Bohemia: magnetic susceptibility logs and their dynamic time warping alignment. *Stratigraphy* **8**, 217–35.

Hofmann, M., Linnemann, U., Gerdes, A., Ullrich, B. & Schauer, M. 2009. Timing of dextral strike-slip processes and basement exhumation in the Elbe Zone (Saxo-Thuringian Zone): the final pulse of the Variscan Orogeny in the Bohemian Massif constrained by LA-SF-ICP-MS U–Pb zircon data. In *Ancient Orogens and Modern Analogues* (eds J. B. Murphy, J. D. Keppie & A. J. Hynes), pp. 197–214. Geological Society of London, Special Publication no. 327.

Hollister, L. S. & Crawford, M. L. 1986. Melt-enhanced deformation: a major tectonic process. *Geology* **14**, 558–61.

Holub, F. V., Cocherie, A. & Rossi, P. 1997. Radiometric dating of granitic rocks from the Central Bohemian Plutonic Complex: constraints on the chronology of thermal and tectonic events along the Barrandian–Moldanubian boundary. *Comptes Rendus de L'Academie des Sciences, Series IIA, Earth and Planetary Science* **325**, 19–26.

Horný, R. 1965. Tectonic structure and development of the Silurian between Beroun and Tachlovice. *Journal for Mineralogy and Geology* **10**, 147–55.

Jamieson, R. A. & Beaumont, C. 2013. On the origin of orogens. *Geological Society of America Bulletin* **125**, 1671–702.

Janoušek, V., Braithwaite, C. J. R., Bowes, D. R. & Gerdes, A. 2004. Magma-mixing in the genesis of Hercynian calc-alkaline granitoids: an integrated petrographic and geochemical study of the Sázava intrusion, Central Bohemian Pluton, Czech Republic. *Lithos* **78**, 67–99.

Janoušek, V. & Gerdes, A. 2003. Timing the magmatic activity within the Central Bohemian Pluton, Czech Republic: conventional U–Pb ages for the Sázava and Tábor intrusions and their geotectonic significance. *Journal of the Czech Geological Society* **48**, 70–1.

Janoušek, V., Wiegand, B. A. & Žák, J. 2010. Dating the onset of Variscan crustal exhumation in the core of the Bohemian Massif: new U–Pb single zircon ages from the high-K calc-alkaline granodiorites of the Blatná suite, Central Bohemian Plutonic Complex. *Journal of the Geological Society, London* **167**, 347–60.

Johnson, M. R. W. 2002. Shortening budgets and the role of continental subduction during the India–Asia collision. *Earth-Science Reviews* **59**, 101–23.

Knížek, M., Melichar, R. & Janečka, J. 2010. Stratigraphic separation diagrams as a tool for determining fault geometry in a folded and thrusted region: an example from the Barrandian region, Czech Republic. *Geological Journal* **45**, 536–43.

Konopásek, J. & Schulmann, K. 2005. Contrasting Early Carboniferous field geotherms: evidence for accretion of a thickened orogenic root and subducted Saxo-thuringian crust (Central European Variscides). *Journal of the Geological Society, London* **162**, 463–70.

Koptíková, L., Bábek, O., Hladil, J., Kalvoda, J. & Slavík, L. 2010. Stratigraphic significance and resolution of spectral reflectance logs in Lower Devonian carbonates of the Barrandian area, Czech Republic; a correlation with magnetic susceptibility and gamma-ray logs. *Sedimentary Geology* **225**, 83–98.

Košler, J., Aftalion, M. & Bowers, D. R. 1993. Mid–late Devonian plutonic activity in the Bohemian Massif: U–Pb zircon isotopic evidence from the Staré Sedlo and Mirotice gneiss complexes, Czech Republic. *Neues Jahrbuch für Mineralogie, Monatshefte* **9**, 417–31.

Košler, J., Bowes, D. R., Farrow, C. M., Hopgood, A. M., Rieder, M. & Rogers, G. 1997. Constraints on the timing of events in the multi-episodic history of the Teplá–Barrandian complex, western Bohemia, from

integration of deformational sequence and Rb–Sr isotopic data. *Neues Jahrbuch für Mineralogie, Monatshefte* **5**, 203–20.

Kroner, U. & Romer, R. L. 2013. Two plates – many subduction zones: the Variscan orogeny reconsidered. *Gondwana Research* **24**, 298–329.

Kříž, J. 1991. The Silurian of the Prague Basin (Bohemia) – tectonic, eustatic and volcanic controls on facies and faunal development. *Special Papers in Palaeontology* **44**, 179–203.

Kříž, J. 1992. Silurian field excursions: Prague Basin (Barrandian), Bohemia. *National Museum of Wales, Geological Notes* **13**, 1–111.

Krs, M., Krsová, M., Pruner, P., Chvojka, R. & Havlíček, V. 1987. Palaeomagnetism, palaeogeography and the multicomponent analysis of Middle and Upper Cambrian rocks of the Barrandian in the Bohemian Massif. *Tectonophysics* **139**, 1–20.

Krs, M., Pruner, P. & Man, O. 2001. Tectonic and paleogeographic interpretation of the paleomagnetism of Variscan and pre-Variscan formations of the Bohemian Massif, with special reference to the Barrandian terrane. *Tectonophysics* **332**, 93–114.

Kubínová, Š., Faryad, S. W., Verner, K., Schmitz, M. D. & Holub, F. V. 2017. Ultrapotassic dykes in the Moldanubian Zone and their significance for understanding of the post-collisional mantle dynamics during Variscan orogeny in the Bohemian Massif. *Lithos* **272–273**, 205–21.

Kukal, Z. & Jäger, O. 1988. Siliciclastic signal of the Variscan orogenesis: the Devonian Srbsko Formation of Central Bohemia. *Bulletin of the Central Geological Survey* **63**, 65–81.

Lease, R. O., Burbank, D. W., Zhang, H., Liu, J. & Yuan, D. 2012. Cenozoic shortening budget for the northeastern edge of the Tibetan Plateau: is lower crustal flow necessary? *Tectonics* **31**, TC3011. doi: 10.1029/2011TC003066.

Lehnert, O., Frýda, J., Buggisch, W., Munnecke, A., Nützel, A., Kříž, J. & Manda, Š. 2007. $\delta^{13}C$ records across the late Silurian Lau event: new data from middle palaeo-latitudes of northern peri-Gondwana (Prague Basin, Czech Republic). *Palaeogeography, Palaeoclimatology, Palaeoecology* **245**, 227–44.

Lewandowski, M. 2003. Assembly of Pangea: combined paleomagnetic and paleoclimatic approach. *Advances in Geophysics* **46**, 199–235.

Li, Y., Wang, C., Dai, J., Xu, G., Hou, Y. & Li, X. 2015. Propagation of the deformation and growth of the Tibetan–Himalayan orogen: a review. *Earth-Science Reviews* **143**, 36–61.

Lister, G. & Foster, M. 2009. Tectonic mode switches and the nature of orogenesis. *Lithos* **113**, 274–91.

Maierová, P., Schulmann, K., Lexa, O., Guillot, S., Štípská, Š., Janoušek, V. & Čadek, O. 2016. European Variscan orogenic evolution as an analogue of Tibetan–Himalayan orogen: insights from petrology and numerical modeling. *Tectonics* **35**, 1760–80.

Manda, Š., Štorch, P., Slavík, L., Frýda, J., Kříž, J. & Tasáryová, Z. 2012. The graptolite, conodont and sedimentary record through the late Ludlow Kozlowskii Event (Silurian) in the shale-dominated succession of Bohemia. *Geological Magazine* **149**, 507–31.

Martínez Catalán, J. R. 2011. Are the oroclines of the Variscan belt related to late Variscan strike-slip tectonics? *Terra Nova* **23**, 241–7.

Martínez Catalán, J. R. 2012. The Central Iberian arc, an orocline centered in the Iberian Massif and some implications for the Variscan belt. *International Journal of Earth Sciences* **101**, 1299–314.

Matte, P. 1986. Tectonics and plate tectonics model for the Variscan belt of Europe. *Tectonophysics* **126**, 329–74.

Matte, P. 2001. The Variscan collage and orogeny (480–290 Ma) and the tectonic definition of the Armorica microplate: a review. *Terra Nova* **13**, 122–8.

Mazur, S. & Aleksandrowski, P. 2001. The Teplá (?)/Saxothuringian suture in the Karkonosze–Izera massif, western Sudetes, central European Variscides. *International Journal of Earth Sciences* **90**, 341–60.

Mazur, S., Aleksandrowski, P., Kryza, R. & Oberc-Dziedzic, T. 2006. The Variscan Orogen in Poland. *Geological Quarterly* **50**, 89–118.

Melichar, R. 2004. Tectonics of the Prague Synform: a hundred years of scientific discussion. *Krystalinikum* **30**, 167–87.

Mikuláš, R. 1998. Ordovician of the Barrandian area: reconstruction of the sedimentary basin, its benthic communities and ichnoassemblages. *Journal of the Czech Geological Society* **43**, 143–59.

Mouthereau, F., Lacombe, O. & Vergés, J. 2012. Building the Zagros collisional orogen: timing, strain distribution and the dynamics of Arabia/Eurasia plate convergence. *Tectonophysics* **532–535**, 27–60.

Murphy, D. C. 1987. Suprastructure/infrastructure transition, east central Cariboo Mountains, British Columbia: geometry, kinematics and tectonic implications. *Journal of Structural Geology* **9**, 13–29.

Paris, F. & Robardet, M. 1990. Early Palaeozoic palaeobiogeography of the Variscan regions. *Tectonophysics* **177**, 193–213.

Patočka, F., Pruner, P. & Štorch, P. 2003. Palaeomagnetism and geochemistry of Early Palaeozoic rocks of the Barrandian (Teplá–Barrandian Unit, Bohemian Massif): palaeotectonic implications. *Physics and Chemistry of the Earth* **28**, 735–49.

Patočka, F. & Štorch, P. 2004. Evolution of geochemistry and depositional settings of Early Palaeozoic siliciclastics of the Barrandian (Teplá–Barrandian Unit, Bohemian Massif, Czech Republic). *International Journal of Earth Sciences* **93**, 728–41.

Pavlis, T. L. 1996. Fabric development in syn-tectonic intrusive sheets as a consequence of melt-dominated flow and thermal softening of the crust. *Tectonophysics* **253**, 1–31.

Pertoldová, J., Verner, K., Vrána, S., Buriánek, D., Štědrá, V. & Vondrovic, L. 2010. Comparison of lithology and tectonometamorphic evolution of units at the northern margin of the Moldanubian Zone: implications for geodynamic evolution in the northeastern part of the Bohemian Massif. *Journal of Geosciences* **55**, 299–319.

Rajlich, P., Schulmann, K. & Synek, J. 1988. Strain analysis of conglomerates in the Central Bohemian shear zone. *Krystalinikum* **19**, 119–34.

Ramsay, J. G. 2003. *Folding and Fracturing of Rocks*. Caldwell, NJ: Blackburn Press, 568 pp.

Ramsay, J. G. 1974. Development of chevron folds. *Geological Society of America Bulletin* **85**, 1741–54.

Riller, U. & Oncken, O. 2003. Growth of the central Andean plateau by tectonic segmentation is controlled by the gradient in crustal shortening. *Journal of Geology* **111**, 367–84.

Robardet, M. 2003. The Armorica 'microplate': fact or fiction? Critical review of the concept and contradictory palaeobiogeographical data. *Palaeogeography, Palaeoclimatology, Palaeoecology* **195**, 125–48.

Röhlich, P. 2007. Structure of the Prague basin: the deformation diversity and its causes (Czech Republic). *Bulletin of Geosciences* **82**, 175–82.

Royden, L. H., Burchfiel, B. C., King, R. W., Wang, E., Chen, Z., Shen, F. & Liu, Y. 1997. Surface deformation and lower crustal flow in eastern Tibet. *Science* **276**, 788–90.

Royden, L. H., Burchfiel, B. C. & van der Hilst, R. D. 2008. The geological evolution of the Tibetan Plateau. *Science* **321**, 1054–8.

Schulmann, K., Konopásek, J., Janoušek, V., Lexa, O., Lardeaux, J. M., Edel, J. B., Štípská, P. & Ulrich, S. 2009. An Andean type Palaeozoic convergence in the Bohemian Massif. *Comptes Rendus Geoscience* **341**, 266–86.

Schulmann, K., Lexa, O., Janoušek, V., Lardeaux, J. M. & Edel, J. B. 2014. Anatomy of a diffuse cryptic suture zone: an example from the Bohemian Massif, European Variscides. *Geology* **42**, 275–8.

Searle, M. P., Elliott, J. R., Phillips, R. J. & Chung, S. L. 2011. Crustal–lithospheric structure and continental extrusion of Tibet. *Journal of the Geological Society, London* **168**, 633–72.

Servais, T. & Sintubin, M. 2009. Avalonia, Armorica, Perunica: terranes, microcontinents, microplates or palaeobiogeographical provinces? In *Early Palaeozoic Peri-Gondwana Terranes: New Insights from Tectonics and Biogeography* (ed. M. G. Bassett), pp. 103–15. Geological Society of London, Special Publication no. 325.

Sláma, J., Dunkley, D. J., Kachlík, V. & Kusiak, M. A. 2008. Transition from island-arc to passive setting on the continental margin of Gondwana: U–Pb zircon dating of Neoproterozoic metaconglomerates from the SE margin of the Teplá–Barrandian Unit, Bohemian Massif. *Tectonophysics* **461**, 44–59.

Slavík, L. 2004. The Pragian–Emsian conodont successions of the Barrandian area: search of an alternative to the GSSP polygnathid-based correlation concept. *Geobios* **37**, 454–70.

Slavík, L., Carls, P., Hladil, J. & Koptíková, L. 2012. Subdivision of the Lochkovian Stage based on conodont faunas from the stratotype area (Prague Synform, Czech Republic). *Geological Journal* **47**, 616–31.

Slobodník, M., Melichar, R., Hurai, V. & Bakker, R. J. 2012. Litho-stratigraphic effect on Variscan fluid flow within the Prague synform, Barrandian: evidence based on C, O, Sr isotopes and fluid inclusions. *Marine and Petroleum Geology* **35**, 128–38.

Stampfli, G. M., Hochard, C., Vérard, C., Wilhem, C. & von Raumer, J. F. 2013. The formation of Pangea. *Tectonophysics* **593**, 1–19.

Štorch, P. 1986. Ordovician–Silurian boundary in the Prague Basin (Barrandian area, Bohemia). *Journal of Geological Sciences, Geology* **41**, 69–103.

Štorch, P. 1990. Upper Ordovician–lower Silurian sequences of the Bohemian Massif, central Europe. *Geological Magazine* **127**, 225–39.

Štorch, P. 2006. Facies development, depositional settings and sequence stratigraphy across the Ordovician–Silurian boundary: a new perspective from the Barrandian area of the Czech Republic. *Geological Journal* **41**, 163–92.

Štorch, P., Fatka, O. & Kraft, P. 1993. Lower Palaeozoic of the Barrandian area (Czech Republic) – a review. *Coloquios de Paleontología* **45**, 163–91.

Štorch, P. & Frýda, J. 2012. The late Aeronian graptolite *sedgwickii* Event, associated positive carbon isotope excursion and facies changes in the Prague Synform (Barrandian area, Bohemia). *Geological Magazine* **149**, 1089–106.

Štorch, P., Manda, Š., Slavík, L. & Tasáryová, Z. 2016. Wenlock–Ludlow boundary interval revisited: new insights from the offshore facies of the Prague Synform, Czech Republic. *Canadian Journal of Earth Sciences* **53**, 666–73.

Strnad, L. & Mihaljevič, M. 2005. Sedimentary provenance of Mid-Devonian clastic sediments in the Teplá–Barrandian Unit (Bohemian Massif): U–Pb and Pb–Pb geochronology of detrital zircons by laser ablation ICP-MS. *Mineralogy and Petrology* **84**, 47–68.

Styron, R. H., Taylor, M. H. & Murphy, M. A. 2011. Oblique convergence, arc-parallel extension, and the role of strike-slip faulting in the High Himalaya. *Geological Society of America Bulletin* **7**, 582–96.

Suchý, V., Dobeš, P., Filip, J., Stejskal, M. & Zeman, A. 2002*a*. Conditions for veining in the Barrandian Basin (Lower Palaeozoic), Czech Republic: evidence from fluid inclusion and apatite fission track analysis. *Tectonophysics* **348**, 25–50.

Suchý, V., Dobeš, P., Sýkorová, I., Machovič, V., Stejskal, M., Kroufek, J., Chudoba, J., Matějovská, L., Havelcová, M. & Matysová, P. 2010. Oil-bearing inclusions in vein quartz and calcite and, bitumens in veins: testament to multiple phases of hydrocarbon migration in the Barrandian basin (lower Palaeozoic), Czech Republic. *Marine and Petroleum Geology* **27**, 285–97.

Suchý, V., Rozkošný, I., Žák, K. & Franců, J. 1996. Epigenetic dolomitization of the Přídolí formation (Upper Silurian), the Barrandian basin, Czech Republic: implications for burial history of Lower Paleozoic strata. *International Journal of Earth Sciences* **85**, 264–77.

Suchý, V., Sandler, A., Slobodník, M., Sýkorová, I., Filip, J., Melka, K. & Zeman, A. 2015. Diagenesis to very low-grade metamorphism in lower Palaeozoic sediments: a case study from deep borehole Tobolka 1, the Barrandian Basin, Czech Republic. *International Journal of Coal Geology* **140**, 41–62.

Suchý, V., Sýkorová, I., Dobeš, P., Machovič, V., Filip, J., Zeman, A. & Stejskal, M. 2012. Blackened bioclasts and bituminous impregnations in the Koněprusy Limestone (Lower Devonian), the Barrandian area, Czech Republic: implications for basin analysis. *Facies* **58**, 759–77.

Suchý, V., Sýkorová, I., Melka, K., Filip, J. & Machovič, V. 2007. Illite 'crystallinity', maturation of organic matter and microstructural development associated with lowest-grade metamorphism of Neoproterozoic sediments in the Teplá–Barrandian unit, Czech Republic. *Clay Minerals* **42**, 503–26.

Suchý, V., Sýkorová, I., Stejskal, M., Šafanda, J., Machovič, V. & Novotná, M. 2002*b*. Dispersed organic matter from Silurian shales of the Barrandian Basin, Czech Republic: optical properties, chemical composition and thermal maturity. *International Journal of Coal Geology* **53**, 1–25.

Tait, J., Bachtadse, V. & Soffel, H. 1994. New palaeomagnetic constraints on the position of central Bohemia during early Ordovician times. *Geophysical Journal International* **116**, 131–40.

Tait, J., Bachtadse, V. & Soffel, H. 1995. Upper Ordovician paleogeography of the Bohemian Massif: implications for Armorica. *Geophysical Journal International* **122**, 211–2018.

Tasáryová, Z., Schnabl, P., Čížková, K., Pruner, P., Janoušek, V., Rapprich, V., Štorch, P., Manda, Š.,

Frýda, J. & Trubač, J. 2014. Gorstian palaeoposition and geotectonic setting of Suchomasty Volcanic Centre (Silurian, Prague Basin, Teplá–Barrandian Unit, Bohemian Massif). *GFF* **136**, 262–5.

Timmermann, H., Dörr, W., Krenn, E., Finger, F. & Zulauf, G. 2006. Conventional and in situ geochronology of the Teplá Crystalline unit, Bohemian Massif: implications for the processes involving monazite formation. *International Journal of Earth Sciences* **95**, 629–47.

Tomek, F., Žák, J. & Chadima, M. 2015. Granitic magma emplacement and deformation during early-orogenic syn-convergent transtension: the Staré Sedlo complex, Bohemian Massif. *Journal of Geodynamics* **87**, 50–66.

Vacek, F. 2011. Palaeoclimatic event at the Lochkovian–Pragian boundary recorded in magnetic susceptibility and gamma-ray spectrometry (Prague Synclinorium, Czech Republic). *Bulletin of Geosciences* **86**, 259–68.

Vanderhaeghe, O. 2012. The thermal–mechanical evolution of crustal orogenic belts at convergent plate boundaries: a reappraisal of the orogenic cycle. *Journal of Geodynamics* **56–57**, 124–45.

Venera, Z., Schulmann, K. & Kroner, A. 2000. Intrusion within a transtensional tectonic domain: the Čistá granodiorite (Bohemian Massif): structure and rheological modelling. *Journal of Structural Geology* **22**, 1437–54.

Verner, K., Buriánek, D., Vrána, S., Vondrovic, L., Pertoldová, J., Hanžl, P. & Nahodilová, R. 2009. Tectonometamorphic features of geological units along the northern periphery of the Moldanubian Zone (Bohemian Massif). *Journal of Geosciences* **54**, 87–100.

Vodrážková, S., Frýda, J., Suttner, T. J., Koptíková, L. & Tonarová, P. 2013. Environmental changes close to the Lower–Middle Devonian boundary; the Basal Choteč Event in the Prague Basin (Czech Republic). *Facies* **59**, 425–49.

Volk, H., Horsfield, B., Mann, U. & Suchý, V. 2002. Variability of petroleum inclusions in vein, fossil and vug cements: a geochemical study in the Barrandian Basin (Lower Palaeozoic, Czech Republic). *Organic Geochemistry* **33**, 1319–41.

Weinerová, H., Hron, K., Bábek, O., Šimíček, D. & Hladil, J. 2017. Quantitative allochem compositional analysis of Lochkovian–Pragian boundary sections in the Prague Basin (Czech Republic). *Sedimentary Geology* **354**, 43–59.

Winchester, J. A. 2002. Palaeozoic amalgamation of Central Europe: new results from recent geological and geophysical investigations. *Tectonophysics* **360**, 5–21.

Yin, A. & Harrison, T. M. 2000. Geologic evolution of the Himalayan–Tibetan orogen. *Annual Review of Earth and Planetary Sciences* **28**, 211–80.

Žák, J., Dragoun, F., Verner, K., Chlupáčová, M., Holub, F. V. & Kachlík, V. 2009. Forearc deformation and strain partitioning during growth of a continental magmatic arc: the northwestern margin of the Central Bohemian Plutonic Complex, Bohemian Massif. *Tectonophysics* **469**, 93–111.

Žák, J., Holub, F. V. & Verner, K. 2005. Tectonic evolution of a continental magmatic arc from transpression in the upper crust to exhumation of mid-crustal orogenic root recorded by episodically emplaced plutons: the Central Bohemian Plutonic Complex (Bohemian Massif). *International Journal of Earth Sciences* **94**, 385–400.

Žák, J., Kraft, P. & Hajná, J. 2013. Timing, styles, and kinematics of Cambro–Ordovician extension in the Teplá–Barrandian Unit, Bohemian Massif, and its bearing on the opening of the Rheic Ocean. *International Journal of Earth Sciences* **102**, 415–33.

Žák, J., Kratinová, Z., Trubač, J., Janoušek, V., Sláma, J. & Mrlina, J. 2011. Structure, emplacement, and tectonic setting of Late Devonian granitoid plutons in the Teplá–Barrandian unit, Bohemian Massif. *International Journal of Earth Sciences* **100**, 1477–95.

Žák, J. & Sláma, J. 2017. How far did the Cadomian 'terranes' travel from Gondwana during early Palaeozoic? A critical reappraisal based on detrital zircon geochronology. *International Geology Review*, published online 5 June 2017. doi: 10.1080/00206814.2017.1334599.

Žák, J., Sláma, J. & Burjak, M. 2017. Rapid extensional unroofing of a granite–migmatite dome with relics of high-pressure rocks, the Podolsko complex, Bohemian Massif. *Geological Magazine* **154**, 354–80.

Žák, J., Verner, K., Holub, F. V., Kabele, P., Chlupáčová, M. & Halodová, P. 2012. Magmatic to solid state fabrics in syntectonic granitoids recording early Carboniferous orogenic collapse in the Bohemian Massif. *Journal of Structural Geology* **36**, 27–42.

Zulauf, G. 1994. Ductile normal faulting along the West Bohemian Shear Zone (Moldanubian/Teplá–Barrandian boundary): evidence for late Variscan extensional collapse in the Variscan Internides. *Geologische Rundschau* **83**, 276–92.

Zulauf, G. 1997. From very low-grade to eclogite-facies metamorphism: tilted crustal sections as a consequence of Cadomian and Variscan orogeny in the Teplá–Barrandian unit (Bohemian Massif). *Geotektonische Forschungen* **89**, 1–302.

Zulauf, G. 2001. Structural style, deformational mechanisms and paleodifferential stress along an exposed crustal section: constraints on the rheology of quartzofeldspathic rocks at supra- and infrastructural levels (Bohemian Massif). *Tectonophysics* **332**, 211–37.

Zulauf, G., Bues, C., Dörr, W. & Vejnar, Z. 2002. 10 km minimum throw along the West Bohemian shear zone: evidence for dramatic crustal thickening and high topography in the Bohemian Massif (European Variscides). *International Journal of Earth Sciences* **91**, 850–64.

Zuza, A. V., Cheng, X. & Yin, A. 2016. Testing models of Tibetan Plateau formation with Cenozoic shortening estimates across the Qilian Shan–Nan Shan thrust belt. *Geosphere* **12**, 501–32.

Zwart, H. J. 1967. The duality of orogenic belts. *Geologie en Mijnbouw* **46**, 283–309.